



Open Archive Toulouse Archive Ouverte



OATAO is an open access repository that collects the work of Toulouse researchers and makes it freely available over the web where possible

This is an author's version published in:

<http://oatao.univ-toulouse.fr/27269>

Official URL

DOI : <https://doi.org/10.1016/j.compchemeng.2020.106853>

To cite this version: Robles, Jesús  and Azzaro-Pantel, Catherine  and Aguilar-Lasserre, Alberto *Optimization of a hydrogen supply chain network design under demand uncertainty by multi-objective genetic algorithms.* (2020) *Computers & Chemical Engineering*, 140. 106853. ISSN 0098-1354

Any correspondence concerning this service should be sent to the repository administrator: tech-oatao@listes-diff.inp-toulouse.fr

Optimization of a hydrogen supply chain network design under demand uncertainty by multi-objective genetic algorithms

Jesus Ochoa Robles^a, Catherine Azzaro-Pantel^{a,*}, Alberto Aguilar-Lasserre^b

^a Université de Toulouse, Laboratoire de Génie Chimique, LGC UMR CNRS 5503 INP UPS TOULOUSE INP ENSIACET - 4 allée Emile Monso – BP 44362 - 31432, Toulouse Cedex 4, France

^b Instituto Tecnológico de Orizaba, Oriente 9, Emiliano Zapata, Orizaba 94320, Ver., Mexico

A B S T R A C T

Hydrogen is currently considered one of the most promising sustainable energy carriers for mobility applications. A model of the hydrogen supply chain (HSC) based on MILP formulation (mixed integer linear programming) in a multi-objective, multi-period formulation, implemented via the ϵ -constraint method to generate the Pareto front, was conducted in a previous work and applied to the Occitania region of France. Three objective functions have been considered, i.e., the levelized hydrogen cost, the global warming potential, and a safety risk index. However, the size of the problem mainly induced by the number of binary variables often leads to difficulties in problem solution. The first innovative part of this work explores the potential of genetic algorithms (GAs) via a variant of the non-dominated sorting genetic algorithm (NSGA-II) to manage multi-objective formulation to produce compromise solutions automatically. The values of the objective functions obtained by the GAs in the mono-objective formulation exhibit the same order of magnitude as those obtained with MILP, and the multi-objective GA yields a Pareto front of better quality with well-distributed compromise solutions. The differences observed between the GA and the MILP approaches can be explained by way of managing the constraints and their different logics. The second innovative contribution is the modelling of demand uncertainty using fuzzy concepts for HSC design. The solutions are compared with the original crisp models based on either MILP or GA, giving more robustness to the proposed approach.

1. Introduction

Hydrogen is one of the most promising energy carriers in the search for a resilient, sustainable energy mix to be used in different applications, such as stationary fuel cell systems and electro-mobility applications.

The challenge of developing a future commercial hydrogen economy involves the deployment of a viable hydrogen supply chain (HSC), considering the most energy-efficient, environmentally benign, safe and cost-effective pathways to deliver hydrogen to the consumer (IEA 2017). The HSC for the mobility market

is defined as a system of activities from suppliers to customers. The activities include the choice of the energy source, production technology, storage, and distribution until reaching refuelling stations. Hydrogen can be produced either centrally (similar to existing gasoline supply chains) or distributed at forecourt refuelling stations as small-scale units that can produce H₂ close to the use point in small quantities.

The network design of the HSC applied to fuel cell electric vehicles has been studied in various works, as highlighted in Table 1. The most common methodology to solving the HSC problems involves a mixed integer linear programming (MILP) approach.

In the same vein, the work conducted in (De-León Almaraz et al., 2014) solved a multi-period model using a deterministic MILP approach embedded in a GAMS/CPLEX environment with a multi-objective formulation implemented via the ϵ -constraint method to generate the Pareto front. The final choice for the HSC was performed through a multiple criteria decision-making process (i.e., technique for order of preference by similarity to ideal solution, TOPSIS). The modelling approach used one economic objective based on hydrogen total daily cost (TDC), one environmental

Acronyms: CCS, Carbon Capture and Storage; GA, Genetic Algorithm; GHG, Greenhouse Gas; GWP, Global Warming Potential; HSC, Hydrogen Supply Chain; MCDM, Multi-Criteria Decision Making; MILP, Mixed Integer Linear Programming; MINLP, Mixed Integer Nonlinear Programming; NSGA-II, Non-dominated Sorting Genetic Algorithm; SCND, Supply Chain Network Design; SMR, Steam Methane Reforming; TDC, Total Daily Cost; TOPSIS, Technique for Order Preference by Similarity to Ideal Solution.

* Corresponding author.

E-mail address: catherine.azzaropantel@ensiacet.fr (C. Azzaro-Pantel).

<https://doi.org/10.1016/j.compchemeng.2020.106853>

Table 1

Territorial approach of the HSC studies.

Approach	Territorial scale	Uncertain parameters	Author(s)	Time scale (periods)		Objective(s)	Energy source	Observations			
				Mono	Multi						
MILP	Great Britain	No	(De León Almaraz, 2014)	X		Cost, Ecological, Safety risk	Natural gas, coal, biomass	ε -constraint method for the multi-period problem The Pareto front is obtained by the ε -constraint method Development of a spatially-explicit MILP model, called SHIPMod (Spatial Hydrogen Infrastructure Mode)			
			(Guillén-Gosálbez et al., 2010)		5 (5 years)	Cost, Ecological					
			(Ren et al., 2007)		9 (2020-2060)	Financial	Coal, Natural gas, Biomass (CCS), renewable				
			(Kim et al., 2011)	x	4 (seasons)		Wind, renewable sources				
			(Deb et al., 2002)				Natural gas, coal, biomass, other renewable sources				
			(Ebrahimnejad and Verdegay, 2016)		5 (2005-2034)						
			(Almansoori and Shah, 2012)		3 (2005-2022)						
			Korea		(Kim et al., 2008)	X				Natural gas, renewable sources	Demand uncertainty is modelled using scenario-based-approach Demand uncertainty is modelled using scenario-based-approach
			Germany	No	(Delgado et al., 1993)	X			Natural gas, Coal (CCS), Biomass		
			Jeju Island, Korea		(McKinsey&Company, 2010)		12 (months)			Biomass	A sensitivity analysis is conducted to provide insights into the efficient management of the biomass-to-hydrogen supply chain ε -constraint method for the multi-period problem The territorial scale is not specified, only defined as a "geographical region"
Midi-Pyrénées, France		(De-León Almaraz et al., 2014)		4 (2010-2050)	Cost, Ecological, Safety risk	Natural gas, photovoltaic, wind, hydro, nuclear					
Regional level		(Bento, 2010)		5 (2004-2038)	Financial, Ecological	Natural gas, coal, biomass, other renewable sources					
China Malaysia		(McKinsey and Company 2010) (Almansoori and Shah, 2006)	x	5 (2010-2034)	Cost	Natural gas, coal, biomass, water electrolysis					
Korea		(Murthy Konda et al., 2011)	X		Financial, Safety	Natural gas, renewable sources	Two methods for demand determination: one based on the prediction of vehicle numbers and the other based on the supply of gasoline and diesel The relative risk index proposed is based on the relative risks of individual components of hydrogen infrastructure				
Spain	Fuel price	(Sabio et al., 2010)		8	Financial, Risk	Natural gas, coal (CCS), Biomass, renewable resources	The uncertainty is associated to the operating costs				
MINLP-GIS Fuzzy multiple objective programming Genetic Algorithms MINLP	Pakistan	No	(Ochoa Robles et al., 2018)	X		Financial	Biomass	The Pareto front is obtained by an adaptive weighted-sum method			
	Korea		(Dagdougui et al., 2012)	X		Financial, Ecological, Risk	Natural gas (CCS), other renewable sources				
	Midi-Pyrénées, France		(Kim and Moon, 2008)		4 (2010-2050)		Natural gas, renewable sources				
	Unspecified		(European Commission 2008)			Financial, Ecological					

objective based on GHG (greenhouse gas) emissions and a safety index.

In this work, as well as in the majority of the works reported in the literature, the economic criterion is formulated as a linear function that has the advantage of simplifying problem solving. Much progress has been made in the solution of the supply chain network design (SCND) models, as emphasized in the work of (Eskandarpour et al., 2015), which analysed the development of efficient multi-objective models that adequately address the different dimensions of sustainable development. Concerning solution techniques, standard and powerful solvers have been the most widely used tools to solve SCND models. However, the size and particularly the number of binary variables in practical supply chain problems often lead to numerical difficulties so that the initial problem must be decomposed into an upper-level master problem, which is a specific relaxation for obtaining a lower bound on the cost, being combinatorially less complex than the original model. The lower level planning problem is typically solved for the selected set of technologies, yielding an upper bound on the total cost of the network for any feasible solution of the upper level (Guillén-Gosálbez et al., 2010).

The results reported in (De-León Almaraz et al., 2014) also showed that the solution strategy based on the ε -constraint method for a multi-objective, multi-period problem is not so straightforward, particularly for the creation of the pay-off tables: the number of the generated efficient solutions can be controlled by properly adjusting the number of grid points in each of the objective function ranges, which can be considered as an asset compared to the weighting method (Mavrotas, 2007) but does not guarantee diversity in the set of solutions.

Over the last decade, there has been a growing interest in genetic algorithms (GAs) to solve a variety of single and multi-objective problems in supply chain management that are combinatorial and NP-hard (Dimopoulos and Zalzalá, 2000, Gen and Cheng, 2000). The first scientific challenge of this work is thus to explore the potential of genetic algorithms (GAs) via a variant of NSGA II (Gomez et al., 2008) to address the combinatorial nature of the HSC design problem and to provide an automatic generation of the Pareto front of the resulting problem.

The second scientific barrier is to model the uncertainty related to different variables and parameters of the HSC, e.g., fuel price (Sabio et al., 2010) or hydrogen demand, which have been identified as among the most significant parameters in the HSC (Ochoa Robles et al., 2015, Ochoa Robles et al., 2017). Several methods have generally been mentioned to model demand uncertainty (Chen and Lee, 2004, Jung et al., 2004, You and Grossmann, 2008): (i) the scenario-based approach; (ii) the distribution-based approach; (iii) the fuzzy-based approach; (iv) the deterministic planning and scheduling models, with the incorporation of safety stock levels; and (v) the spatially aggregated demand model.

As far as HSC is concerned, significant work in this field was performed by (Kim et al., 2008) who developed a steady-state, stochastic MILP model to consider the effect of hydrogen demand uncertainty. A scenario planning approach to capture uncertainty in hydrogen demand over a long-term planning horizon was developed in (Almansoori and Shah, 2012, Nunes et al., 2015). Although stochastic methods are traditionally used, they are generally time consuming and might not represent the nature of uncertainty since the problem of hydrogen supply chain design can be viewed as a deployment problem for which data collection for demand is not possible for a new product development problem. This reason motivates our choice to use an alternative approach based on fuzzy concepts (Verdegay, 1982, Villacorta et al., 2017).

A comprehensive review of studies in the field of SCND (supply chain network design) and reverse logistics network design under uncertainty was recently developed (Govindan et al., 2017) and

showed that a few studies applied meta-heuristics approaches. Due to the NP-hard nature of the SCND problem under uncertainty, developing this type of solution approach can be viewed as a promising alternative. Although meta-heuristics cannot guarantee the optimal solution for an optimization problem, these approaches can solve large-scale problems within an acceptable computation time.

This paper first presents the methods and tools used for the development of an HSC design framework with uncertain hydrogen demand. The adaptation of the model previously developed in (De-León Almaraz et al., 2014) is presented. A comparison between the results is obtained by the two models for a multi-objective case based on the minimization of the total daily cost (TDC), global warming potential (GWP) and safety risk (Risk), measured by the relative risk of hydrogen activities proposed in (Kim et al., 2008). For this purpose, a case study developed for the French market of the Occitania region (partially corresponding to the former Midi-Pyrénées region) solved by the initial MILP model is used to validate the new methodology. Occitania's ambition is to become the first Positive Energy Region in Europe, and it is committed to cutting in half its energy consumption per capita, which is the equivalent of a 40% reduction in the energy consumption of the region and to multiplying by three its renewable energy production, both by 2050: the use of hydrogen could be one solution to reaching this target. A 3-echelon supply chain involving hydrogen production, transportation and storage in the territory, divided into 8 sub-regions, is considered. Some significant results are highlighted and compared with those previously obtained with crisp values.

2. Methods and tools

2.1. General principles of HSC framework design with uncertain demand

The general methodology of the HSC design proposed in this work is illustrated in Fig. 1. It shows the extended flow diagram of the methodology proposed for HSC design optimization, considering both the multi-objective optimization framework either based on the deterministic MILP solution strategy developed in (De León Almaraz, 2014) or on a GA and the multiple criteria decision making tool selected to find the most interesting solution from the compromise solutions obtained from the Pareto front based on a variant of the TOPSIS method (Ren et al., 2007). The MULTI-GEN environment previously developed in our research group [8] was selected as the genetic algorithm platform. The demand uncertainty has been modelled using fuzzy concepts as presented in (Verdegay, 1982, Villacorta et al., 2017).

2.2. Capturing the HSC design model in a GA environment

The mathematical model previously developed by (De León Almaraz, 2014) for HSC design was solved within the GAMS 23.9 environment using CPLEX solver. This model has been adapted to be embedded in an external optimization loop based on the multi-objective genetic algorithm. The whole model is presented to maintain its integrity, and the changes that have been adopted to consider the integration into the external optimization loop are presented in italics.

2.2.1. HSC modelling principles

A general supply chain network (SCN) model for hydrogen (see Fig. 2) is considered (production plants, storage units, distribution grids and demand for each grid).

The following assumptions have been made:

- The number of grids is known (8);
- The capacity of the production plants and the storage plants is known;

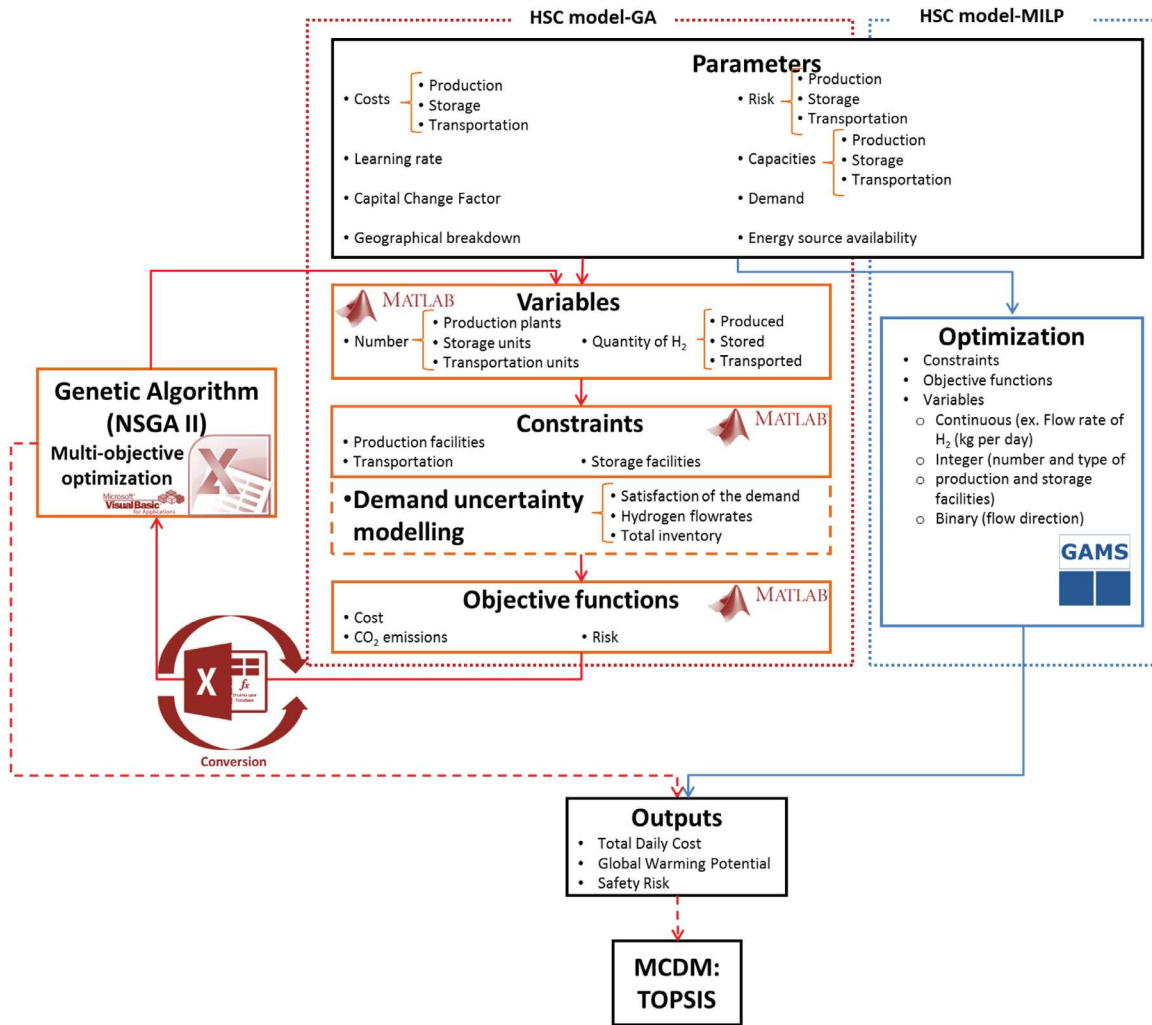


Fig. 1. Methodology of the HSC design framework.

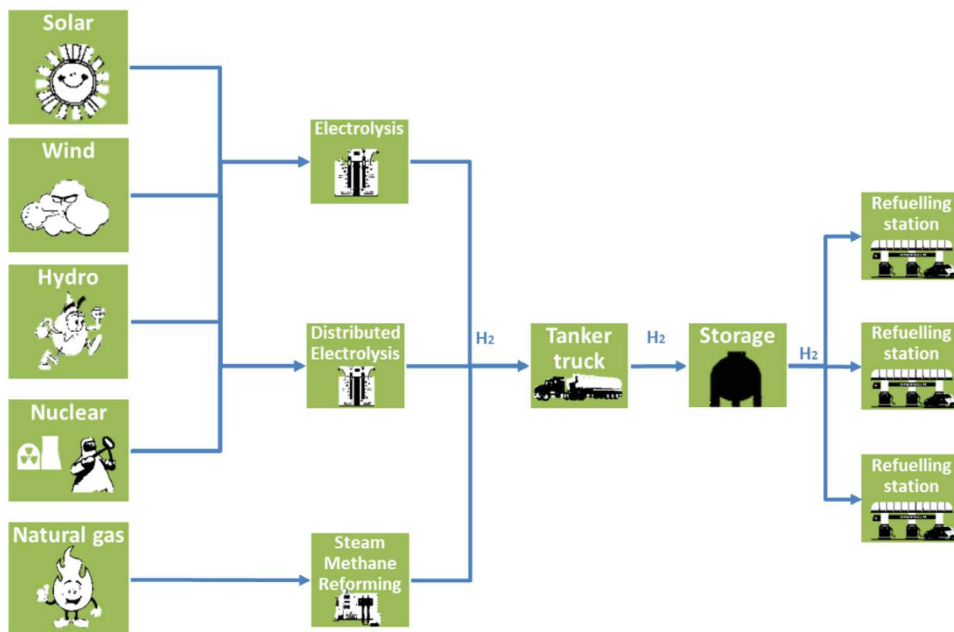


Fig. 2. Supply chain network model.

Table 2
Optimization variables and dependent variables.

Optimization variables	Dependent variables			
NP_{pig}	AH_{ig}	GC	PGWP	TCC
NSS_{ig}	DI_{ig}	GWP_{tot}	PT_{ig}	TDC
PR_{pig}	DL_{ig}	LC	RP_{ig}	TGWP
$Q_{ilgg'}$	FC	MC	SGWP	
	FCC	$NTU_{ilgg'}$	SP_{ig}	
	FOC	PD_{ig}	ST_{ig}	

- The demand for each one of the grids is fixed and known (for the crisp model);
- It is possible to either import or export hydrogen from/to each grid;
- Each grid can produce hydrogen in three different ways, i.e., steam methane reforming (SMR), electrolysis (centralized) and distributed electrolysis (decentralized, i.e., produced onsite for captive uses); and
- The average distance between the main cities is considered to calculate the delivery distances over the road network.

The mathematical model formulation involves the following notations:

- g and g' : grid squares such that $g' \neq g(8)$
- i : product physical form (LH₂)
- l : type of transportation modes (tanker truck)
- p : plant type with different production technologies (SMR, electrolysis, diselectrolysis)
- s : storage facility type with different storage technologies (LH₂ stock)
- e : energy source type (natural gas, solar, wind, hydroelectric, nuclear)

The model formulation is developed in the Appendix. The design decisions are based on the number, type, capacity, and location of production and storage facilities, the number of transport units, and the flow rate of hydrogen between locations. The operational decisions concern the total production rate of hydrogen in each grid, the total average inventory in each grid, the demand covered by imported hydrogen and local production.

The involved constraints are related to demand satisfaction, the availability of energy sources, production facilities, storage units, transportation modes and flow rates.

The variables used in this model are split into two groups: decision variables that are generated by the optimization procedure; and dependent variables that are calculated from the equality constraints. The classification is shown in Table 2.

2.3. Multi-objective optimization by GAs

The solving method used in this investigation is based on a multi-objective genetic algorithm. Let us recall that, in a single-objective optimization, the optimal solution is usually clearly defined. However, this assumption is not the case for a multi-objective problem in which the objectives can conflict. A single solution is hardly the best for all of the objectives simultaneously. Instead of a single optimum, there is a set of trade-off solutions, which are the so-called Pareto optima solutions. The aim of the multi-objective evolutionary algorithm is to cause the solution set

to approach the Pareto ideal frontier of the problem with a wide and uniform distribution in a single simulation run.

A variant of the non-dominated sorting genetic algorithm II (NSGA-II) (Deb et al., 2002), which is one of the most widely used multi-objective evolutionary algorithms implemented through the MULTIGEN library developed by (Gomez et al., 2008), was selected in this work.

The main feature of NSGA-II among multi-objective evolutionary techniques is the determination of individual fitness values based on the Pareto dominance relationship and density information between individuals.

In this work, the results obtained from the ϵ -constraint method (De León Almaraz, 2014) and GA are compared to analyse the advantages and disadvantages of each technique and its impact on the network configuration of the HSC. The set of chromosomes representing the variables is illustrated in Fig. 3.

The variable PR represents the production rate of product i by plant type p in grid g ; Q is the flow rate of product i by transport l between the grids g and g' . NP is the number of production plants of type p of product i in grid g , while NS is the number of storage facilities of type p of product i in grid g . Finally, DL is the demand satisfied for product i by local production in grid g . In the GA used, the chromosome of the variables is complemented by a vector containing the type of variable (i.e., 0 for continuous variables, 1 for integer variables and 2 for binary variables). The other procedures follow the NSGAI variant proposed by (Gomez et al., 2008).

2.4. Multiple criteria decision making (MCDM)

A modified TOPSIS (M-TOPSIS) evaluation is based on the original concept of TOPSIS (technique for order of preference by similarity to ideal solution) and proposed by (Ren et al., 2007) is used. It chooses an alternative that should simultaneously have the closest distance from the positive ideal solution and the farthest distance from the negative ideal solution, solving the rank reversal and the evaluation failure problem presented in the original TOPSIS technique.

2.5. Uncertainty modelling

2.5.1. Fuzzy-constraint problems

The review proposed by (Ebrahimnejad and Verdegay, 2016) has reported that many works have been devoted to fuzzy linear programming (FLP) and solution methods. These works are typically divided into four areas: (FLP1) linear programming (LP) problems with fuzzy inequalities and crisp objective function; (FLP2) LP problems with crisp inequalities and fuzzy objective function; (FLP3) LP problems with fuzzy inequalities and fuzzy objective function; and (FLP4) LP problems with fuzzy parameters. In the HSC design problem that has been mathematically formulated (De León Almaraz, 2014), hydrogen demand has been identified as an uncertain parameter, and the HSC design problem refers to the simplest form of fuzzy linear programming, i.e., FLP1.

The decision maker can accept a violation of the constraints up to a certain degree previously established. This acceptance can be formalized for each constraint as (Villacorta et al., 2017):

$$a_i x \leq_f b_i, \quad i = 1, \dots, m$$

Production rate				Flow rate				Production plants				Storage facilities			
PR_{111}	PR_{112}	...	PR_{pig}	Q_{111}	Q_{112}	...	$Q_{ilgg'}$	NP_{111}	NP_{112}	...	NP_{pig}	NS_{111}	NS_{112}	...	NS_{pig}

Fig. 3. Chromosome of the GA model.



Fig. 4. Uncertain demand modelling.

In this expression, the f index indicates that the inferior relationship involves fuzzy numbers.

This index can be modelled using a membership function:

$$\mu_i : R \rightarrow [0, 1], \mu_i(x) = \begin{cases} 1 & \text{if } x \leq b_i \\ f_i(x) & \text{if } b_i \leq x \leq b_i + t_i \\ 0 & \text{if } x \geq b_i + t_i \end{cases}$$

where the f_i are continuous, non-increasing functions. The tolerance that the decision maker is willing to accept up to a value of $b_i + t_i$ is given by the membership function μ_i . For every $x \in R$, $\mu_i(x)$ represents the degree of fulfilment of the i -th constraint. Then, the problem can be solved:

$$\max z = cx$$

subject to

$$Ax \leq_f b$$

$$x \geq 0$$

The approach proposed by (Verdegay, 1982) through the representation theorem has proved that the problem can be solved via the following parametric linear programming problem:

$$\max z = cx$$

subject to

$$Ax \leq g(\alpha)$$

$$x \geq 0, \alpha \in [0, 1]$$

where $g(\alpha) = (g_1(\alpha), \dots, g_m(\alpha)) \in R^m$, with $g_i = f_i^{-1}$.

To simplify the problem, if f_i are linear:

$$\max z = cx$$

subject to

$$Ax \leq b + t(1 - \alpha)$$

$$x \geq 0, \alpha \in [0, 1]$$

with $t = (t_1, \dots, t_m) \in R^m$.

It has been proved (Delgado et al., 1993) that, when f_i is linear, a solution for the fuzzy constraints problem can be found as if it is a model with non-linear functions, without any generality loss when assuming linear functions for the fuzzy constraints. Some sample values can be applied to α in the interval $[0,1]$, and then the model can be solved for every sample value. For example, a step size of 0.25 for sampling α can be transformed in five α -cuts for $\alpha = \{0; 0.25; 0.5; 0.75; 1\}$.

2.5.2. Application to demand uncertainty modelling in HSCN design

Hydrogen demand is the only parameter that will be considered uncertain. In this paper, only the modifications implemented in the HSC model are presented (see Fig. 4).

The uncertainty has been considered using the following information:

- The lower and upper levels of demand have been obtained from the analysis in (De León Almaraz, 2014);
- From these values, average demand is calculated;

- The difference between the average and the low/high demand is calculated, representing an accepted tolerance; and
- Variable α is then introduced. This variable can take values from 1 to 0, and it represents the rate of use of tolerance. A value of α equal to 0.5 corresponds to the average demand.

The constraints that are modified in the initial crisp version of the model are constraints 2-4.

Considering the demand as the right side of the constraints, as in Verdegay's approach (Verdegay, 1982), the fuzzy right side can be expressed mathematically as:

$$\widetilde{DT}_{ig} = [DT_{ig} + PD_{ig}(1 - \alpha)] \quad (1)$$

Eq. (1) must be inserted into constraints (2)-(4), which replace the corresponding ones in the initial model (see (De León Almaraz, 2014)).

$$DL_{ig} + DI_{ig} = DT_{ig} + PD_{ig}(1 - \alpha) \quad \forall i, g \quad (2)$$

$$PT_{ig} - \sum_{l, g'} (Q_{ilgg'} - Q_{ilgg'g}) = DT_{ig} + PD_{ig}(1 - \alpha) \quad \forall i, g \quad (3)$$

$$\frac{ST_{ig}}{\beta} = DT_{ig} + PD_{ig}(1 - \alpha) \quad \forall i, g \quad (4)$$

PD_{ig} is the tolerance of DT_{ig} , and α is the rate of use of the tolerance. Six values of α -cuts were considered: $\alpha = \{0.16; 0.33; 0.5; 0.66; 0.83; 1\}$. For each value of α -cuts, an evaluation of the model was performed.

3. Case study

3.1. Parameters of the HSC

3.1.1. Estimation of hydrogen demand

The case study refers to the design for an HSC in the former Midi-Pyrénées region in France as previously presented in (De León Almaraz, 2014). The demand is considered deterministic for the first case and is calculated from the work of (McKinsey&Company, 2010) with the same methodology as proposed in (De-León Almaraz et al., 2014). The demand evolution profile corresponds to the values of D_{\min} (Table 3) (low demand scenario studied in (De-León Almaraz et al., 2014)). The demand (for both D_{\min} and D_{\max}) includes fuel cell electric vehicles and captive fleets (i.e., buses, private and light-goods vehicles, forklifts) as defined in (De León Almaraz, 2014). The market demand scenarios are established from (Bento, 2010) and (McKinsey and Company 2010), in which the two scenarios identifying the two levels of demands for FCEV penetration were developed providing the

Table 3
Demand scenarios of FCEV penetration.

Scenario/year	2020	2030	2040	2050
D_{\min}	1%	7.5%	17.5%	25%
D_{\max}	2%	15%	35%	50%

Table 4
Demand (D_{min} , D_{max}) and tolerance (PD) evolution profile used in the case study (kg per day).

Period/Grid	1			2			3			4		
	Dmin	Dmax	PD	Dmin	Dmax	PD	Dmin	Dmax	PD	Dmin	Dmax	PD
2020	502	995	493	843	1650	807	977	1953	976	709	1404	695
2030	3780	7440	3660	6320	12430	6110	7410	14630	7220	5320	10450	5130
2040	8850	17350	8500	14750	29030	14280	17330	34100	16770	12400	24380	11980
2050	12610	24790	12180	21100	41470	20370	24770	48730	23960	17710	34810	17100
Period/Grid	5			6			7			8		
	Dmin	Dmax	PD	Dmin	Dmax	PD	Dmin	Dmax	PD	Dmin	Dmax	PD
2020	570	1136	566	639	1263	624	3221	6362	3141	437	810	373
2030	4420	8590	4170	4850	9510	4660	24180	47670	23490	3150	6250	3100
2040	10260	20030	9770	11310	22160	10850	56470	111230	54760	7420	14570	7150
2050	14610	28610	14000	16170	31660	15490	80620	158950	78330	10580	20790	10210

percentage of FCEV expected to replace ICEs (ignition combustion engines).

The hydrogen demand for the two scenarios is obtained from Eq. (5) (Almansoori and Shah, 2006), (Murthy Konda et al., 2011):

$$DT_{ig} = (FE)(d)(Qc_g) \quad (5)$$

where the total demand in each grid (DT) is provided by the fuel economy of the vehicle (FE), the average distance travelled (d) and the number of FCEVs in each grid (Qc).

For uncertain demand, Table 4 also presents the demand in the high demand scenario case proposed by (De-León Almaraz et al., 2014), i.e., (D_{max}). The tolerances are represented by the differences between D_{max} and D_{min} over the periods.

3.1.2. Techno-economic assumptions

The study is based on the following assumptions:

- a capital change factor (depreciation period) of 12 years is introduced;
- in a multi-period approach, four periods were analysed, from 2020 to 2050, with a 10-year time step for each;
- three types of technologies to produce hydrogen are considered: steam methane reforming (SMR), electrolysis and distributed electrolysis;
- five energy sources are considered: solar, wind, hydro, nuclear and natural gas (Ochoa Robles et al., 2018);
- hydrogen must be liquefied before being stored or distributed;
- a minimum capacity of production and storage equal to 50 kg of H_2 per day is considered;
- renewable energy is directly used on site because of grid saturation, which allows to allocate the CO_2 impact on each source;
- one size for storage and production units is considered;
- inter-district transport is allowed;
- the maximum capacity of transportation is fixed at 3500 kg liquid- H_2 (Dagdougui et al., 2012);
- the hydrogen is stored in liquid form, and a 10-day LH_2 safety stock is considered;
- the risk index is calculated by the methodology proposed by (Kim and Moon, 2008);
- the number of plants is initialized at a null value;

- the cost of switching from a current refuelling station to H_2 fuel is not considered; and
- the learning rate cost reductions due accumulated experience is considered as 10% per period (McKinsey and Company 2010).

3.2. Optimization parameters

For the mono-period and mono-objective case, a total of 500 individuals in the population and 1000 generations are considered, with 0.9 for the crossover rate and 0.5 for the mutation rate. These values have been fixed from a preliminary sensitivity analysis. As already highlighted, the definition of variables is different in both models. In the GA formulation, there are 352 decision variables versus 676 in the MILP formulation. In the case of multi-period and multi-objective formulations, 2000 individuals in the population and 3000 generations are used, with 1408 variables versus 3319 in the MILP model. For the M-TOPSIS analysis (Ren et al., 2007), the same weighting factors for cost, safety, and environmental criteria are considered. The default feasibility of CPLEX and the optimality tolerances of 10^{-6} have been adopted.

4. Results

In Sections 4.1 to 4.3, the same cost data as those used in (De-León Almaraz et al., 2014) are adopted for validation purposes. The parameters of the HSC model are presented in the supplementary materials. In all of the maps provided, the number of plants is indicated inside the symbols used for technology representation. The maps are obtained after the successive use of the optimization algorithm and the MCDM strategy for the multi-objective case.

For the mono-period optimization runs (Sections 4.1 and 4.2), the demand scenario relative to period 4 is analysed.

4.1. Mono-objective and mono-period optimization

A preliminary study was performed with the GA approach: 10 runs were performed for each case to guarantee the stochastic nature of the algorithm (Table 5). The same methodology is used for all of the cases in which the GA methodology is used.

Table 5
Statistical results of the runs performed in the mono-period and mono-objective GA approach.

	Min (TDC)			Min (GWP)			Min (Risk)		
	TDC (M\$/ day)	GWP (ton CO_2 eq / day)	Risk	TDC (M\$ / day)	GWP (ton CO_2 eq per day)	Risk	TDC (M\$ / day)	GWP (ton CO_2 eq / day)	Risk
Mean	1.21	1552.08	496	1.32	763.42	485	1.22	1642.82	479
Standard deviation	0.0327	257.38	21.17	0.0218	167.42	22.17	0.0251	211.80	11.98

Table 6
Mono-objective and mono-period detailed optimization results.

Objective	MILP (CPLEX)			GA		
	TDC	GWP	Risk	TDC	GWP	Risk
Demand (t per day)	198.2					
Number of total production facilities	24	402	25	27	27	25
Number of total storage facilities	214	214	214	214	214	214
Number of transport units	6	0	0	14	13	12
<i>Capital cost</i>						
Plants and storage facilities (10 ⁶ \$)	169.11	297.35	179.5	207.31	260.3	211.5
Transportation modes (10 ⁶ \$)	1.4	0	0	6.5	5.0	6.0
<i>Operating cost</i>						
Plants and storage facilities (10 ³ \$ per day)	793.57	1289.78	792.68	729.27	729.27	733.73
Transportation modes (10 ³ \$ per day)	2.29	0	0	4.91	4.27	3.97
Total daily cost (10 ⁶ \$ per day)	1.18	1.97	1.2	1.21	1.32	1.22
Cost per kg H₂ (\$)	5.95	9.94	6.05	6.10	6.66	6.16
Production facilities (t CO ₂ -eq per day)	1999.30	614.33	2001.50	1401.47	614.33	1493.45
Storage facilities (t CO ₂ -eq per day)	139.51	139.51	139.51	139.51	139.51	140.45
Transportation modes (t CO ₂ -eq per day)	4.91	0	0	11.09	9.58	8.9175
Total GWP (t CO ₂ -eq per day)	2143.72	753.84	2141.01	1552.08	763.42	1642.82
Kg CO₂-eq per kg H₂	10.82	3.80	10.80	7.83	3.85	8.29
Production facility risk	11.82	110.10	12.96	15.99	15.90	14.73
Storage facility risk	387	387	387	390.6	390.6	390.6
Transportation modes risk	35.1	0	0	89.1	78.0	73.5
Total Risk	433.92	497.10	399.96	495.64	484.50	478.78

The results of the three mono-objective optimizations (min TDC, GWP, and Risk separately), solved by CPLEX, on the one hand, and by the GA, on the other hand, are presented in Table 6. For each criterion to be optimized, each column presents the optimized values of the decision variables, some intermediate values involved in the evaluation of the criteria and the optimized value of the considered criterion (in bold type and in colour). For each mono-optimization case, a computation of the other criteria is also performed in parallel.

Table 6 also presents the unit cost of H₂ as well as the amount of emitted CO₂ per kg of H₂ that is deduced from the value of the optimization criteria (in the same colour).

It can be observed that, whichever criterion is considered, CPLEX outperforms GA.

For instance, when TDC is minimized, a lower value is not surprisingly obtained with CPLEX (1.18 M\$/day) than with GA (1.21 M\$/day), which is exactly the same trend with the other criteria.

Let us consider once more the TDC case minimization for the sake of illustration. Since a better value has been obtained with MILP for TDC, the value of GWP is now higher than that obtained with GA (respectively, 10.82 kg CO₂-eq per kg H₂ with MILP vs 7.83 kg CO₂-eq per kg H₂ with GA), reflecting a compromise among the criteria. This type of observation is not valid in this case for the risk criterion, which can be explained by different use of transport between the grids.

The trend observed for TDC can be generalized to the other criteria: it means that, if a better value is systematically obtained with MILP than with GA for a given criterion that has been optimized, the performance of one criterion that is not optimized can be degraded compared to the results obtained with GA in the same conditions.

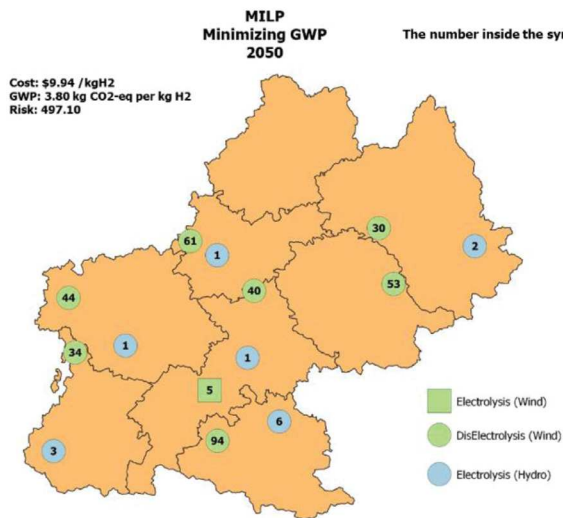
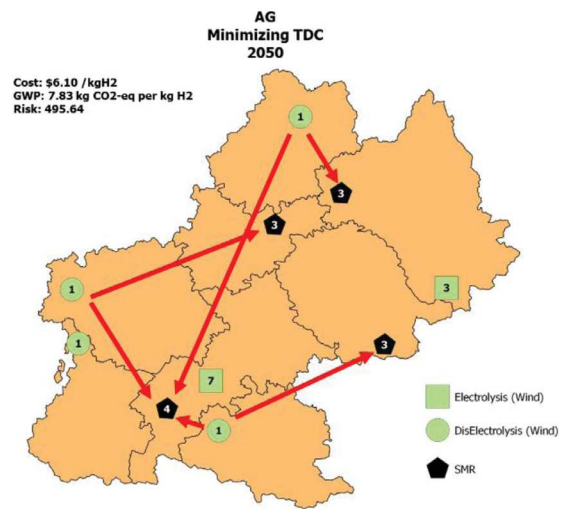
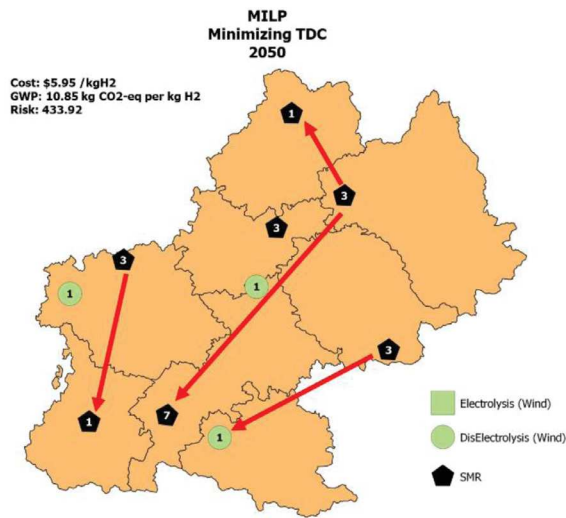
Fig. 5 shows the obtained network for the three optimization cases. For TDC minimization, the networks obtained are very close to each other with both optimization strategies, producing the most hydrogen via SMR with some electrolysis plants. The main

difference between the approaches mostly involves the way in which hydrogen is distributed through the grids.

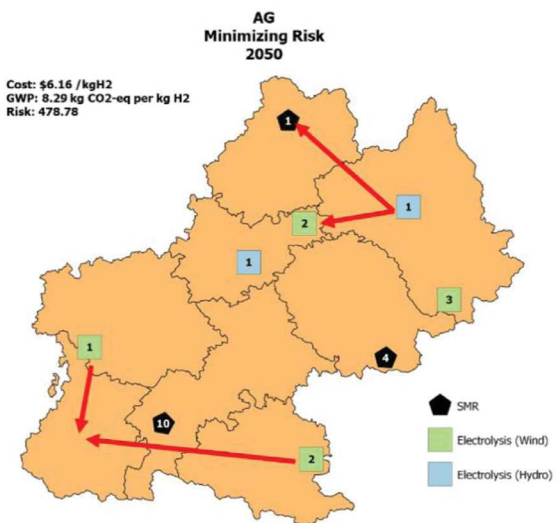
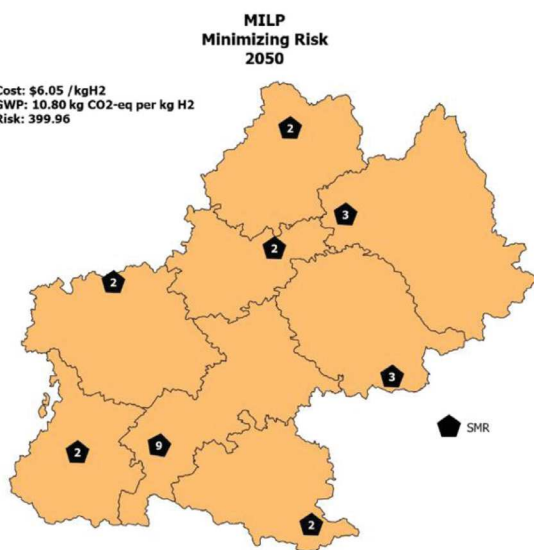
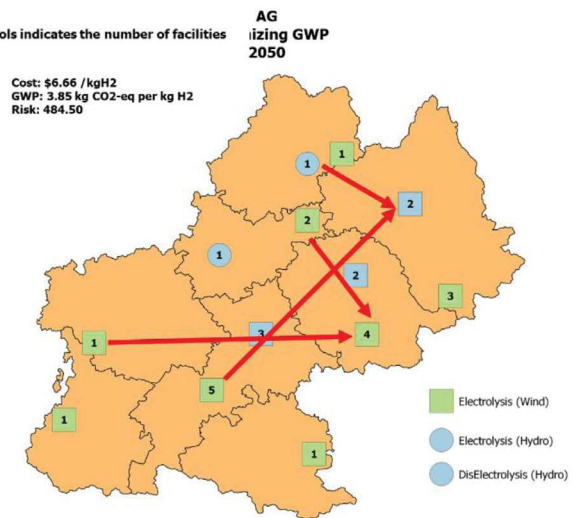
When GWP is minimized, priority is given to the production of hydrogen via electrolysis for both approaches. With the MILP model, there is no transport between grids, and hydrogen production is achieved through several distributed plants. With GA, fewer facilities are installed, but hydrogen transportation occurs through grids.

Table 7
Best trade-off solutions selected by TOPSIS for ε -constraint and AG.

	MILP	GA
Demand (t per day)	198.17	198.17
Number of total production facilities	25	39
Number of total storage facilities	214	214
Number of transport units	0	0
<i>Capital cost</i>		
Plants and storage facilities (10 ⁶ \$)	2595.00	2480.45
Transportation modes (10 ⁶ \$)	0	0
<i>Operating cost</i>		
Plants and storage facilities (10 ³ \$ per day)	1056.20	1143.28
Transportation modes (10 ³ \$ per day)	0	0
Total daily cost (10 ⁶ \$ per day)	1.65	1.68
Cost per kg H₂ (\$)	8.32	8.48
Production facilities (t CO ₂ -eq per day)	614.33	409.82
Storage facilities (t CO ₂ -eq per day)	139.51	139.51
Transportation modes (t CO ₂ -eq per day)	0	0
Total GWP (t CO ₂ -eq per day)	753.84	549.33
Kg CO₂-eq per kg H₂	3.80	2.77
Production facility risk	14.40	16.05
Storage facility risk	387.00	387
Transportation modes risk	0	0
Total Risk	401.40	403.05

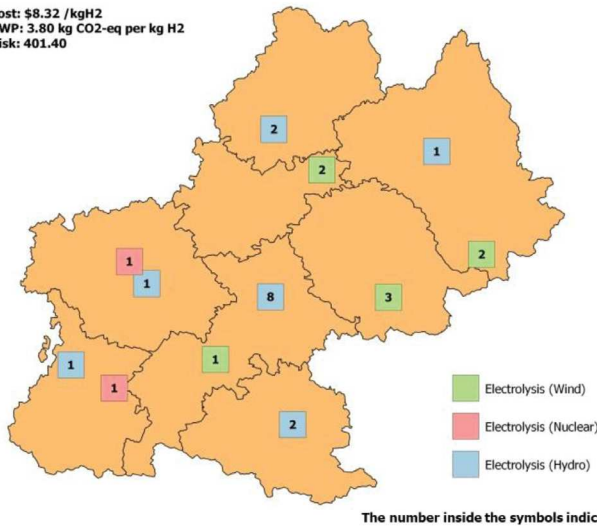


The number inside the symbols indicates the number of facilities



The number inside the symbols indicates the number of facilities
MILP
Multi-objective and mono-period

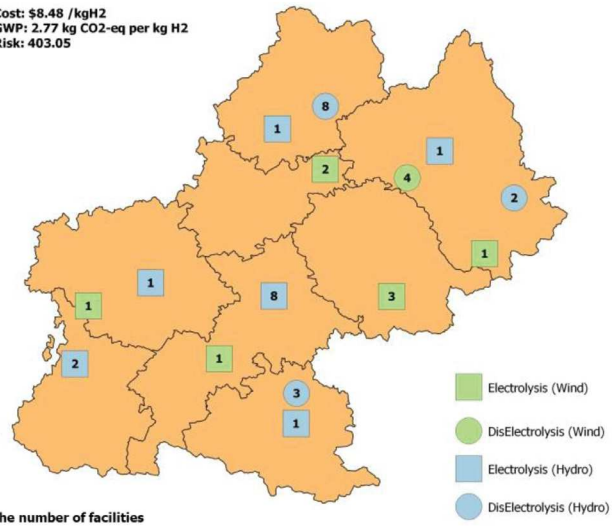
Cost: \$8.32 /kgH2
 GWP: 3.80 kg CO2-eq per kg H2
 Risk: 401.40



a)

GA
Multi-objective and mono-period

Cost: \$8.48 /kgH2
 GWP: 2.77 kg CO2-eq per kg H2
 Risk: 403.05



b)

Fig. 6. Maps of the two scenarios with multi-objective optimization a) with GA; b) with MILP.

For risk minimization, hydrogen production is based exclusively on SMR plants for the MILP approach and a mix of SMR and electrolysis for the GA approach with transportation through grids. This situation is mainly due to the small difference in the risk values between the various technologies for the plant size that is considered.

It must be emphasized that the solar source is eliminated in the optimization process since hydrogen produced via electrolysis with solar energy is the most expensive process and exhibits a higher carbon footprint, compared to wind and hydro.

4.2. Multi-objective and mono-period optimization

In this case, the obtained results are only slightly improved with linear programming, compared to GA for cost and risk criteria (Table 7, Fig. 6 (a) and (b)). The degree of centralization is almost the same. In Fig. 6 (a), relative to GA, the configuration involves a set of several plants with the distributed electrolysis technology with no transportation; with MILP in Fig. 6 (b), priority is given to electrolysis plants from various sources, including the nuclear one (see Table 8).

The Pareto solutions proposed by the GA include the Pareto space, which was identified as using the MILP methodology (Fig. 7). A small variation (2%) is observed in the unit cost (\$8.32 of MILP vs \$8.48 per kg H₂ of GA) between the two TOPSIS solutions. From the environmental viewpoint, a significant improvement is observed with the GA: GWP expressed in kg CO₂ eq per kg H₂ in the GA approach is 27% lower than the value obtained with the

Table 8
 Use ratio of energy sources for hydrogen production (multi-objective and mono-period case).

Energy source	MILP	GA
Wind	60%	69%
Hydraulic	32%	31%
Nuclear	8%	0%

MILP approach. This difference can be explained by the use of distributed plants instead of electrolysis plants. The difference in the risk criteria between the approaches is not significant.

The computation time for MILP with CPLEX (Intel® Xeon® CPU 2.10GHz) is approximately 3 hours versus 4 hours with GA, with a set of 174 Pareto points obtained with the GA approach and 43 with the MILP approach.

4.3. Multi-objective and multi-period optimization

Fig. 8 is a projection of the Pareto surface onto the two-dimensional plane corresponding to cost and environmental impact. For these two criteria, better compromise solutions are obtained with the GA than with CPLEX. This case is not true with the risk index, which can be higher.

The TOPSIS solutions (see Table 9) provide lower values for both cost and GWP. The unit cost of hydrogen is lower with GA (8.00) than with MILP (8.27), despite a slightly higher risk (838 vs 873). This outcome can be explained by the way in which the plants are distributed through the periods.

In the MILP approach (Fig. 9), priority is given in the first period to the establishment of distributed plants, mainly due to the low value of the demand. In the three other periods, the demand is satisfied mainly with the electrolysis plants so that GWP and risk remain not as high.

In the GA approach (Fig. 9), the first period is dedicated to the installation of distributed electrolysis plants and one SMR, significantly increasing CO₂ emissions. For the second period, some electrolysis plants are added. The CO₂ emissions remain higher than with MILP, and because of transport between grids, the risk also increases. For the third and fourth periods, transport between grids remains, but the SMR plants disappear from distribution, decreasing the CO₂ emissions.

Finally, for this example and without providing a feature of generality to the obtained results, compared to MILP, GA promotes the deployment of hydrogen by favouring cost objectives in the first period. In the last two periods, better values for GWP are obtained with the GA approach rather than with MILP because of the instal-

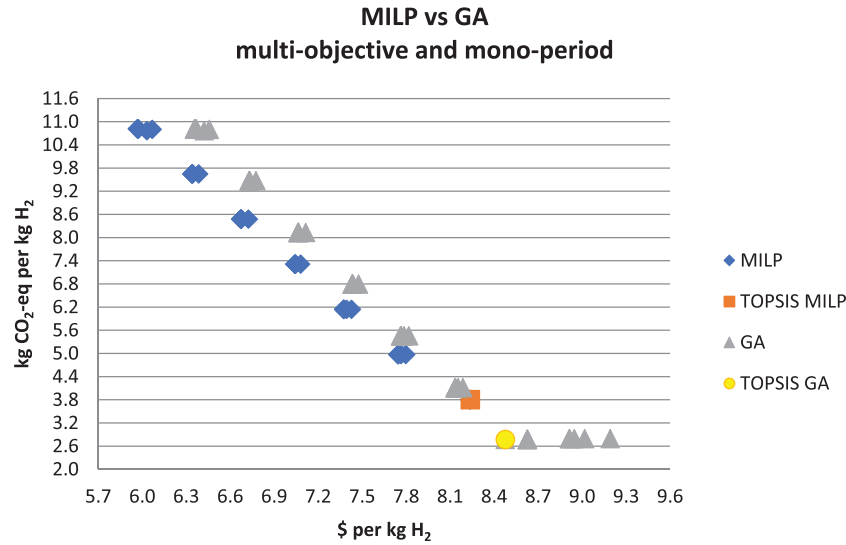


Fig. 7. Pareto fronts for the optimization carried out by MILP and GA.

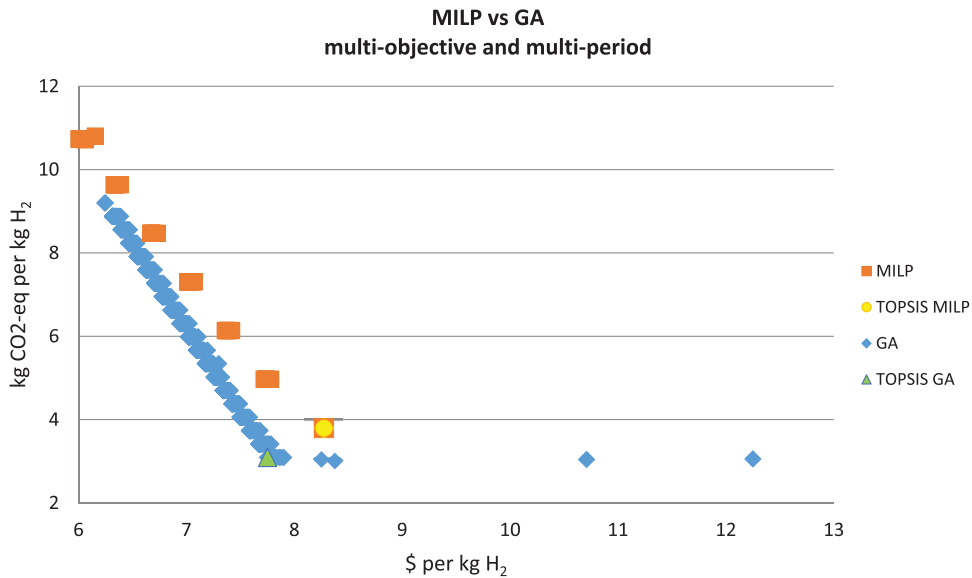


Fig. 8. Projection of the Pareto fronts onto the two-dimensional plane corresponding to cost and environmental impact for the optimization run carried out by MILP and GA for a multi-objective and multi-period approach.

lation of a smaller number of production facilities. This approach leads again to the implementation of transport between grids to satisfy the demand. Finally, from the safety point of view (risk), the MILP model presents better results, mostly due to the absence of transport between the grids. Table 10 shows the percentage of energy sources used by each methodology. Regarding the mono-objective case, the solar source is eliminated in the optimization process.

4.4. Multi-objective and multi-period optimization with new costs

In addition to hydrogen demand, one of the most significant parameters is feedstock cost (Ochoa Robles et al., 2017), (Ochoa Robles et al., 2017). In the original model (De-León Almaraz et al., 2014), the unit production cost (UPC) of electricity remains fixed for all of the periods regardless of the technology, which was a severe simplification. In what follows, an evaluation of UPC is considered with fixed facility costs (maintenance, labour cost), as well as electricity and feedstock costs.

Table 11 presents the price of electricity produced from different energy sources and the price of natural gas for conditions in France (2013).

In the original model, UPC is a fixed parameter (De León Almaraz, 2014) (SMR: \$3.36 per kg; electrolysis: \$4.69 per kg; dis-electrolysis \$6.24per kg), which is only dependent on the size of the production unit (\$ per kg H₂). However, as mentioned in the (McKinsey&Company, 2010) report, a better vision of UPC is to consider the fixed, electricity and feedstock costs. The fixed cost is related to labour and maintenance.

All of the contributions are reflected in Eq. (6), where the UPC calculation (\$ per kg H₂) is given by the addition of the fixed cost of a production plant of type *p* and size *j* in time period *t* (FCP_{ept}, \$ per kg H₂), the electricity cost for general usage in a production plant of type *p* projected for time period *t* (EC_{ept}, \$ per kg H₂) and the feedstock *e* cost for a production plant of the *p* type (FSC_{ept}). The FSC_{ept} is obtained by multiplying the feedstock *e* efficiency in the process *p* in time *t* (kWh_{elec}/kg H₂) by the feedstock *e* price (\$/kWh_{elec}), and for the electrolysis process, the feedstock consid-

Table 9
Multi-objective and multi-period optimization results.

	MILP				GA			
	2020	2030	2040	2050	2020	2030	2040	2050
Year								
Demand (t per day)	7.90	59.43	138.79	198.17	7.90	59.43	138.79	198.17
Number of total production facilities	17	34	47	69	17	28	30	41
Number of total storage facilities	12	66	150	214	12	66	150	214
Number of transport units	0	0	0	0	0	4	2	3
<i>Capital cost</i>								
Plants and storage facilities (10 ⁶ \$)	681.01	765.69	707.92	185.42	737.93	520.31	443.72	153.42
Transportation modes (10 ⁶ \$)	0	0	0	0	0	0.80	0.28	0.41
<i>Operating cost</i>								
Plants and storage facilities (10 ³ \$ per day)	49.35	321.64	748.23	1066.00	48.14	332.99	786.41	1133.53
Transportation modes (10 ³ \$ per day)	0	0	0	0	0	1.31	0.46	0.46
Total daily cost (10 ³ \$ per day)	91.68	525.60	1127.00	1600.25	83.17	476.53	1116.65	1557.90
Cost per kg H ₂ (\$)	11.61	8.84	8.12	8.08	10.53	8.02	8.05	7.86
Production facilities (t CO ₂ -eq per day)	24.58	185.23	430.25	613.33	42.20	220.70	287.02	409.82
Storage facilities (t CO ₂ -eq per day)	5.56	41.84	96.71	139.51	5.56	41.84	97.71	139.51
Transportation modes (t CO ₂ -eq per day)	0	0	0	0	0	2.60	2.19	1.44
Total GWP (t CO ₂ -eq per day)	30.14	226.07	526.96	752.84	47.76	265.13	386.91	550.77
Kg CO ₂ -eq per kg H ₂	3.81	3.80	3.79	3.79	6.05	4.46	2.79	2.78
Production facility risk	4.05	6.30	12.45	16.05	3.96	4.68	9.60	13.50
Storage facility risk	20.7	118.8	272.7	387	20.7	118.8	272.7	387
Transportation modes risk	0	0	0	0	0	20.8	6.5	14.3
Total Risk	24.75	125.10	285.15	403.05	24.66	144.28	288.80	414.80
Global TDC (M\$ per day)			3.34				3.23	
Global unit cost (\$ per kg H ₂)			8.27				8.00	
Global GWP (T CO ₂ eq per day)			1536				1251	
Global Kg CO ₂ -eq per kg H ₂			3.80				3.09	
Global Risk			838				879	

Table 10
Use ratio of energy sources for hydrogen production (multi-objective and multi-period case).

Energy source	MILP				GA			
	2020	2030	2040	2050	2020	2030	2040	2050
Natural gas	0%	0%	0%	0%	6%	11%	0%	0%
Hydro	53%	71%	70%	64%	53%	67%	70%	64%
Wind	41%	24%	30%	36%	41%	22%	30%	36%
Nuclear	6%	6%	0%	0%	0%	0%	0%	0%

Table 11
Prices of natural gas and costs of electricity from different sources (2013).

Energy source (Price/unit)	2020	2030	2040	2050	Reference
European price of natural gas (\$2010/kg)	0.587	1.300	1.750*	2.200	For 2030 and 2050: [48]
Cost of electricity (nuclear) in France (\$2013/kWh)	0.0439	0.0665	0.089*	0.112*	For 2020: [49] For 2030: [50]
Cost of electricity (PV) in France (\$2013/kWh)	0.328	0.101	0.060*	0.053	For 2020: [49] For 2030 and 2050: [51]
Cost of electricity (Wind) in France (\$2013/kWh)	0.073	0.068*	0.063*	0.058	For 2020: [49] For 2050: [51]
Cost of electricity (Hydro) in France (\$2013/kWh)	0.018	0.044*	0.071*	0.098	

* Calculated by interpolation.

ered is electricity, and the energy source cost varies depending on the type, e.g., fossil vs renewable (Table 11).

$$UPC_{e,p,t} = FCP_{e,p,t} + EC_{e,p,t} + FSC_{e,p,t} \quad (6)$$

The feedstock cost is likely to gain importance because it depends on the energy transition scenario and induces a cost change in renewable energy impacting the hydrogen cost over the long-time horizon from 2020 to 2050.

The new UPC calculated for the model is presented in Table 12, in which hydrogen produced via electrolysis with solar energy is

the most expensive, while hydrogen produced with electrolysis from a hydraulic source is less expensive.

The optimization runs are performed with these new costs, and the results are compared with the previous ones (see Fig. 10). A strong decrease in GWP is observed for the range of these new costs, globally leading to better solutions for all criteria.

In the first period (see Fig. 11 and Table 13), the distributed plants are the main sources of production, while in the other periods, the electrolysis plants started to be installed in the different grids. Additionally, there is no transport between grids, and the CO₂ emissions for the plants installed remain very low. Most of

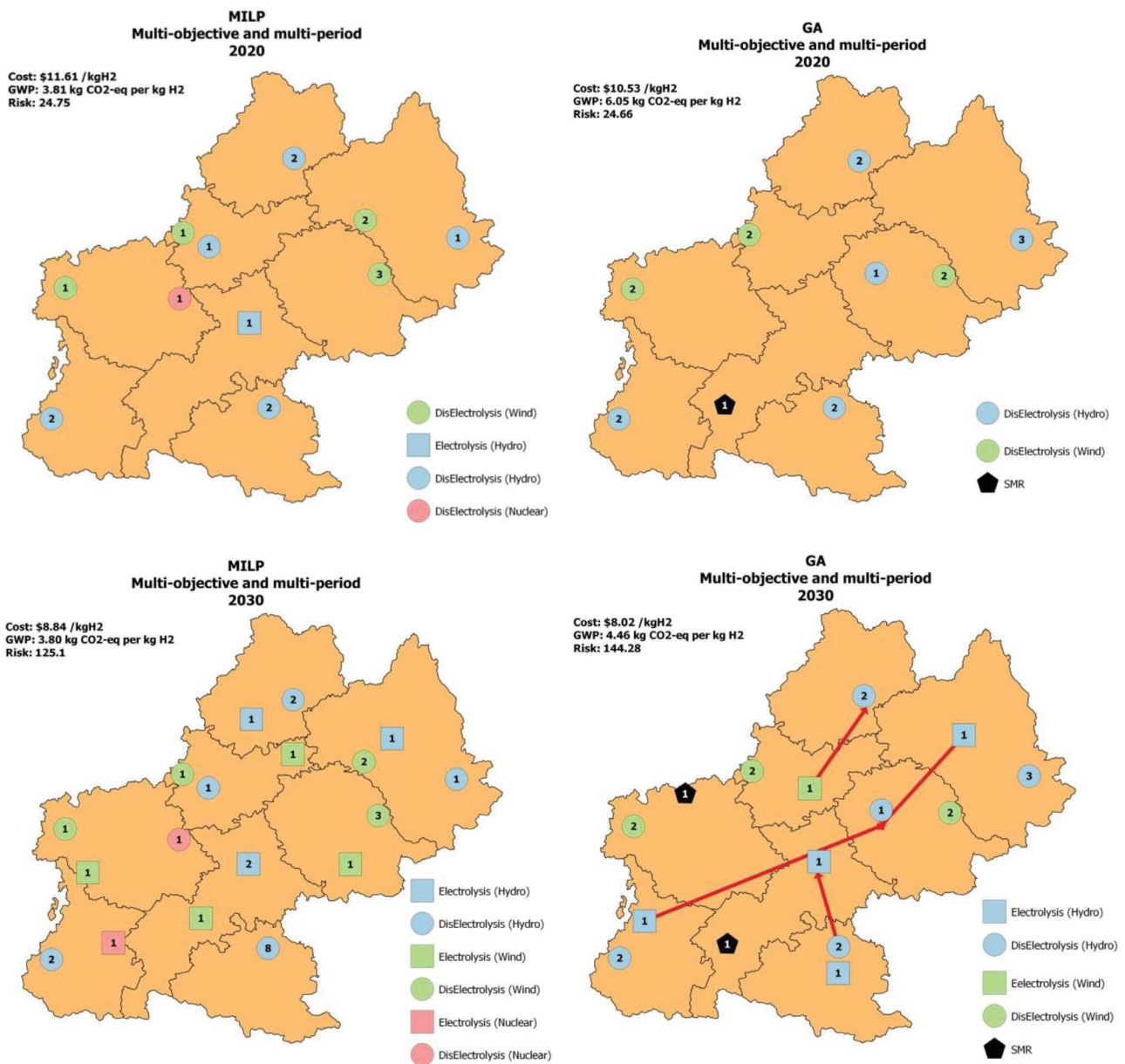


Fig. 9. Maps of the four scenarios for the optimization run carried out by MILP and GA for a multi-objective and multi-period approach.

Table 12

UPC calculated with the new costs.

Production technology	Fixed cost of production (\$ per kg H ₂)	Electricity usage of production plant (\$ per kg H ₂)	Feedstock cost for production plant (\$ per kg H ₂)	Electrical need to produce a kg of H ₂ (kWh _{elec} /kg H ₂)	Cost of energy source (\$ per kg H ₂) [*]				UPC (\$ per kg H ₂)				
					2020	2030	2040	2050	2020	2030	2040	2050	
SMR		0.16	0.02		4.02 [■]	3.71	2.61	3.46	4.62	3.89	2.79	3.64	4.80
Electrolysis	PV	0.39		0.06	55	18.04	5.56	3.30	2.93	18.49	6.01	3.75	3.38
	Wind	0.39		0.06	55	4.00	3.72	3.45	3.17	4.45	4.17	3.90	3.62
	Hydro	0.39		0.06	55	0.98	2.44	3.90	5.36	1.43	2.89	4.35	5.81
	Nuclear	0.39		0.06	55	2.41	3.66	4.90	6.14	2.86	4.11	5.35	6.59
Dis Electrolysis	PV	0.75		0.11	55	18.04	5.56	3.30	2.93	18.90	6.42	4.16	3.79
	Wind	0.75		0.11	55	4.00	3.72	3.45	3.17	4.86	4.58	4.31	4.03
	Hydro	0.75		0.11	55	0.98	2.44	3.90	5.36	1.84	3.30	4.76	6.22
	Nuclear	0.75		0.11	55	2.41	3.66	4.90	6.14	3.27	4.52	5.76	7.00

^{*}[Energy source cost (\$/KWh)x Electrical need to produce a kg of H₂ (kWh_{elec}/kg H₂)].

[■] kg/kg H₂.

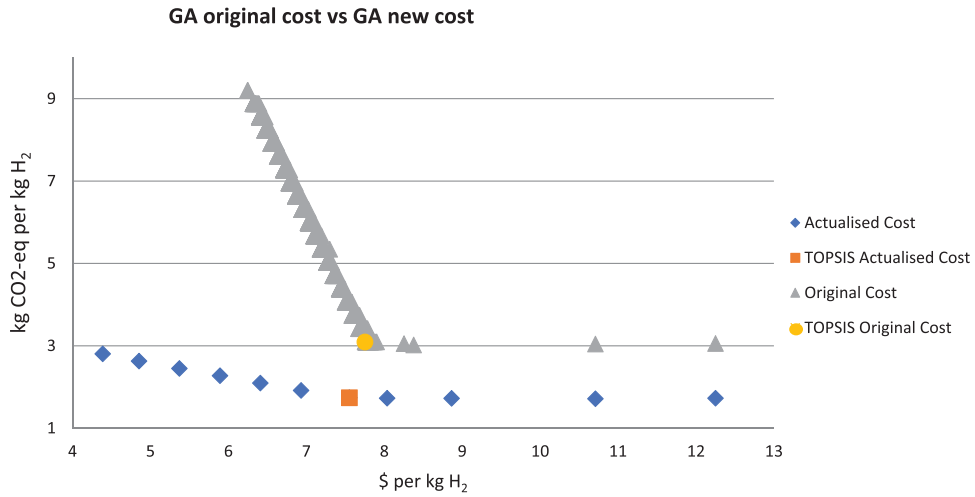
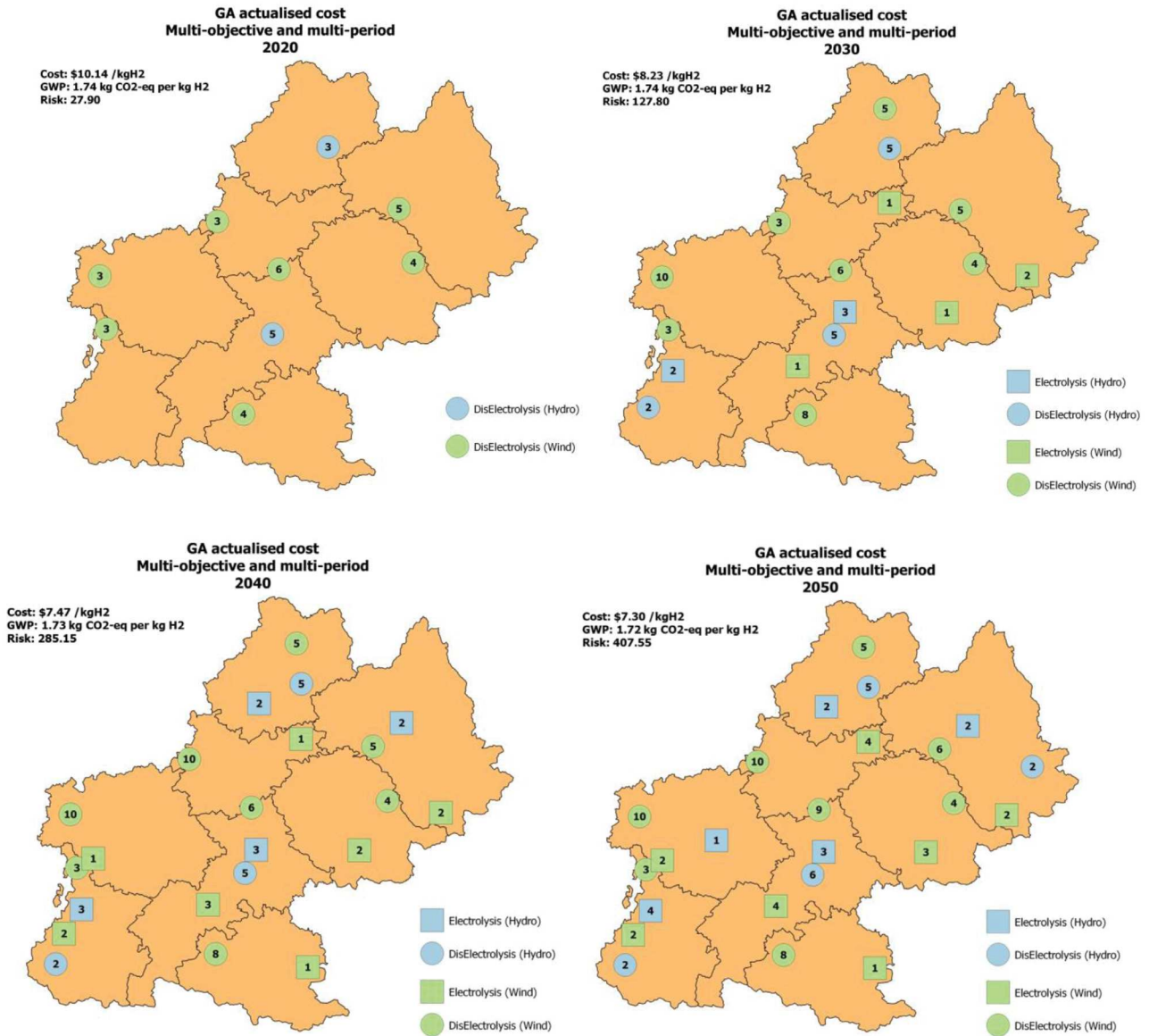


Fig. 10. Pareto fronts obtained with the original GA and the GA with the new cost.



The number inside the figures indicates the number of facilities

Fig. 11. Maps of the GA approach with the new cost model.

Table 13
Multi-objective and multi-period results for actualised costs.

Year	GA new costs			
	2020	2030	2040	2050
Demand (t per day)	7.90	59.43	138.79	198.17
Number of total production facilities	25	62	92	110
Number of total storage facilities	12	66	150	214
Number of transport units	0	0	0	0
<i>Capital cost</i>				
Plants and storage facilities (10 ⁶ \$)	304.47	401.53	263.71	43.44
Transportation modes (10 ⁶ \$)	0	0	0	0
<i>Operating cost</i>				
Plants and storage facilities (10 ³ \$ per day)	43.44	307.15	708.68	1013.16
Transportation modes (10 ³ \$ per day)	0	0	0	0
Total daily cost (10 ³ \$ per day)	80.12	489.34	1036.96	1446.56
Cost per kg H ₂ (\$)	10.14	8.23	7.47	7.30
Production facilities (t CO ₂ -eq per day)	8.27	61.35	142.51	201.91
Storage facilities (t CO ₂ -eq per day)	5.56	41.84	97.71	139.51
Transportation modes (t CO ₂ -eq per day)	0	0	0	0
Total GWP (t CO ₂ -eq per day)	13.73	103.18	240.22	341.42
Kg CO ₂ -eq per kg H ₂	1.74	1.74	1.73	1.72
Production facility risk	7.20	9.00	12.45	20.55
Storage facility risk	20.7	118.8	272.7	387.0
Transportation modes risk	0	0	0	0
Total Risk	27.90	127.80	285.15	407.55
Global TDC (M\$ per day)			3.05	
Global unit cost (\$ per kg H ₂)			7.55	
Global GWP (T CO ₂ eq per day)			698	
Global Kg CO ₂ -eq per kg H ₂			1.73	
Global Risk			848	

Table 14
Use ratio of energy sources for hydrogen production (with new costs).

Energy sources	2020	2030	2040	2050
Hydro	22%	30%	22%	33%
Wind	78%	70%	78%	67%

the energy sources used stem from wind, with almost 70% of the electricity produced (Table 14).

4.5. Multi-objective GA approach under uncertain demand

In this case, the demand can vary between low and high demand (Dmin and Dmax, respectively, in Table 4). The tolerance is

the difference between the two levels of demand, and α is the percentage of tolerance that is added to the base demand (Dmin). Several values of α are used (see Table 15), and the demand used for each α -cut depends on the tolerance level.

For each α -value, a tri-criterion optimization procedure with the GA procedure is implemented, leading to the set of solutions constituting the Pareto front, to which the M-TOPSIS procedure is then applied. The criteria (average values over the periods) relative to the compromise solution of the HSCN finally obtained are presented in Table 16, and the instances obtained for α equal to 0; 0.16; 0.33; and 0.50 are shown in Table 17, in which the relative deviation relative to the case α equal to 0 case is presented.

Table 15
Values of the demand according to the α -cut.

	0.00				α 0.16				0.33			
	2020	2030	2040	2050	2020	2030	2040	2050	2020	2030	2040	2050
Tolerance (t per day)	0.00	0.00	0.00	0.00	1.23	9.21	21.45	30.66	2.53	18.99	44.24	63.24
Demand (t per day)	7.90	59.43	138.79	198.17	9.13	68.64	160.24	228.83	10.43	78.42	183.03	261.41
	0.50				α 0.66				0.83			
	2020	2030	2040	2050	2020	2030	2040	2050	2020	2030	2040	2050
Tolerance (t per day)	3.84	28.77	67.03	95.82	5.07	37.98	88.48	126.48	6.37	47.76	111.27	159.06
Demand (t per day)	11.74	88.20	205.82	293.99	12.96	97.41	227.27	324.65	14.27	107.19	250.06	357.23
	α 1.00											
	2020	2030	2040	2050								
Tolerance (t per day)	7.68	57.54	134.06	191.64								
Demand (t per day)	15.57	116.97	272.85	389.81								

Table 16
Results of HSCN solutions the different α -cuts (average values over the period).

	α value					
	0.16	0.33	0.5	0.66	0.83	1
TDC (M\$ per day)	3.21	3.23	3.42	3.55	3.64	3.74
Relative deviation (reference $\alpha=0$)	5%	6%	12%	16%	19%	23%
Unit cost (\$ per kg H ₂)	6.88	6.06	5.71	5.36	5	4.7
Relative deviation (reference $\alpha=0$)	9%	20%	24%	29%	34%	38%
GWP (T CO ₂ eq per day)	851.2	910.41	1355.8	1870.7	2050.8	2227.5
Relative deviation (reference $\alpha=0$)	22%	30%	94%	168%	194%	219%
GWP (kg CO ₂ eq per kg H ₂)	1.82	1.9	2.65	2.82	2.81	2.8
Relative deviation (reference $\alpha=0$)	5%	10%	53%	63%	62%	62%
Risk	1324	1742.29	1989.7	2210.5	2268.7	2332.3
Relative deviation (reference $\alpha=0$)	56%	105%	135%	161%	168%	175%

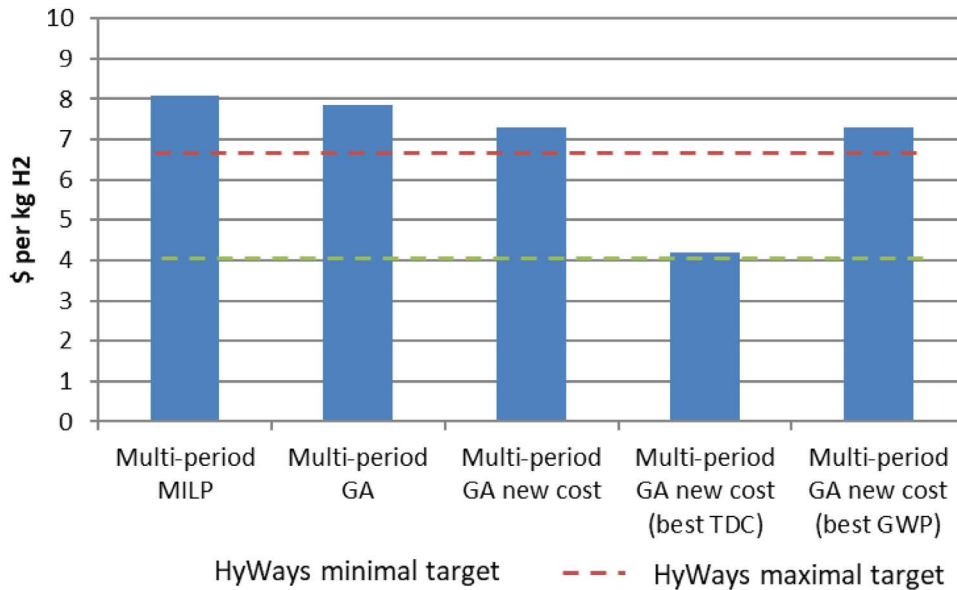
Table 17
Optimal HSCN configurations obtained with $\alpha=0$, $\alpha=0.16$, $\alpha=0.33$ and $\alpha=0.50$.

Year	2020				2030				2040				2050			
Tolerance	0	1.23	2.53	3.84	0	9.21	18.99	28.77	0	21.45	44.24	67.03	0	30.66	63.24	95.82
Demand (t per day)	7.9	9.13	10.43	11.74	59.43	68.64	78.42	88.20	138.79	160.24	160.24	183.03	198.17	228.83	228.83	228.83
Number of total production facilities	25	26	29	21	62	62	63	37	92	92	93	67	110	115	112	111
relative deviation (reference $\alpha=0$)		4%	16%	16%	0%	2%	40%		0%	1%	27%		5%	2%	1%	
Number of total storage facilities	12	13	15	16	66	69	71	76	150	159	163	165	214	225	231	244
relative deviation (reference $\alpha=0$)		8%	25%	33%	5%	8%	15%		6%	9%	10%		5%	8%	14%	
Number of transport units	0	0	0	0	0	0	0	0	0	0	0	0	0	0	0	0
<i>Capital cost</i>																
Plants and storage facilities (10 ⁶ \$)	304.47	318.54	322.25	379.96	401.53	374.15	507.95	570.81	263.71	358.93	432.04	449.53	43.44	100.84	156.77	181.53
relative deviation (reference $\alpha=0$)		5%	6%	25%	7%	27%	42%		36%	64%	70%		132%	261%	318%	
Transportation modes (10 ⁶ \$)	0	0	0	0	0	0	0	0	0	0	0	0	0	0	0	0
<i>Operating cost</i>																
Plants and storage facilities (10 ³ \$ per day)	43.44	46.52	57.82	60.42	307.15	330.33	408.68	508.98	708.68	762.81	950.54	1186.97	1013.16	1090.44	1352.59	1495.63
relative deviation (reference $\alpha=0$)		7%	33%	39%	8%	33%	66%		8%	34%	67%		8%	34%	48%	
Transportation modes (10 ³ \$ per day)	0	0	0	0	0	0	0	0	0	0	0	0	0	0	0	0
Total daily cost (10 ³ \$ per day)	80.12	83.20	93.61	111.86	489.34	512.52	543.11	633.28	1036.96	1091.08	1080.94	1252.52	1446.56	1523.84	1516.56	1537.16
relative deviation (reference $\alpha=0$)		4%	17%	40%	5%	11%	29%		5%	4%	21%		5%	5%	6%	
Cost per kg H ₂ (\$)	10.14	9.12	8.97	9.53	8.23	7.47	6.93	7.18	7.47	6.81	6.75	6.84	7.3	6.66	6.63	6.72
relative deviation (reference $\alpha=0$)		10%	11%	6%	9%	16%	13%		9%	10%	8%		9%	9%	8%	
Production facilities (t CO ₂ -eq per day)	8.27	10.80	13.15	23.28	61.35	79.10	96.22	173.96	142.51	186.80	194.16	345.31	201.91	255.91	261.45	408.20
relative deviation (reference $\alpha=0$)		31%	59%	181%	29%	57%	184%		31%	36%	142%		27%	29%	102%	
Storage facilities (t CO ₂ -eq per day)	5.56	6.08	6.91	7.92	41.84	46.80	53.97	59.56	97.71	106.30	111.30	139.00	139.51	159.45	173.24	198.54
relative deviation (reference $\alpha=0$)		9%	24%	43%	12%	29%	42%		9%	14%	42%		14%	24%	42%	
Transportation modes (t CO ₂ -eq per day)	0	0	0	0	0	0	0	0	0	0	0	0	0	0	0	0
Total GWP (t CO ₂ -eq per day)	13.83	17.28	20.89	33.44	103.18	126.31	151.05	235.78	240.22	293.50	305.97	486.15	341.42	415.77	435.22	608.18

Table 18

Robustness analysis of the optimal configurations.

	$\alpha=0.33$				$\alpha=0.66$				$\alpha=1$			
	2020	2030	2040	2050	2020	2030	2040	2050	2020	2030	2040	2050
TDC (M\$ per day)	89.24	514.66	1083.21	1494.42	93.31	554.59	1193.17	1614.67	98.93	593.65	1292.13	1729.73
Relative deviation (reference $\alpha=0$)	11%	5%	4%	3%	16%	13%	15%	12%	23%	21%	25%	20%
Unit cost (\$ per kg H ₂)	11.30	8.66	7.80	7.54	11.81	9.33	8.60	8.15	12.52	9.99	9.31	8.73
relative deviation (reference $\alpha=0$)	11%	5%	4%	3%	16%	13%	15%	12%	24%	21%	25%	20%
GWP (T CO ₂ eq per day)	13.83	103.19	240.22	341.42	13.85	103.51	241.02	341.98	13.74	102.96	240.52	341.55
relative deviation (reference $\alpha=0$)	0%	0%	0%	0%	0%	0%	0%	0%	1%	0%	0%	0%
GWP (kg CO ₂ eq per kg H ₂)	1.74	1.74	1.73	1.72	1.75	1.74	1.74	1.73	1.74	1.73	1.73	1.72
relative deviation (reference $\alpha=0$)	0%	0%	0%	0%	1%	0%	0%	0%	0%	0%	0%	0%
Risk	45.25	278.12	602.26	821.36	70.31	326.36	749.19	1064.64	94.76	373.11	764.79	1099.59
relative deviation (reference $\alpha=0$)	62%	118%	111%	102%	152%	155%	163%	161%	240%	192%	168%	170%

**Fig. 12.** Cost of hydrogen in 2050 (\$ per kg H₂).

As expected, the operating cost and the capital cost increase with hydrogen demand. Although the TDC is higher when α increases, the unit cost decreases, mostly due to the effect of scale. For example, in the first period (2020), with a value of α equal to 0 (respectively 0.5), the unit cost of H₂ is \$10.14/kg H₂ (respectively \$6.98/kg H₂). The same situation is observed over the whole period. Conversely, GWP and risk increase with hydrogen demand.

The number of facilities also increases as α -value increases, except for α equal to 0.5, for which priority is given to electrolysis plants instead of distributed ones, allowing for greater capacity to be available.

A robustness study can thus be performed from the optimization results presented in Table 18. Let us consider the HSCN configuration obtained with α equal to 0.33. The network, which has been obtained from the successive use of the multi-objective optimization procedures and MCDM techniques, is perfectly consistent with the corresponding demand. However, if the demand does not reach the maximal expected value, it will result in higher values for all criteria. To check whether an acceptable range for the criteria values can still be obtained even if the network is overdimensioned for this demand level, a post-optimal analysis is then performed using the given network and the lowest value of the demand. Table 18 compares the results obtained in both scenarios.

4.6. Results and discussion

The hydrogen price evolution is directly dependent on production and distribution costs. The different studies have shown the

hydrogen cost evolution with the gradual introduction of demand from the mobility sector. A comparative study of the different results considering different FCV market penetration rates, considering different hydrogen production technology choices, was carried out, and even for the highest demand, the results show (see Fig. 12) that hydrogen costs for 2050 remain expensive compared to the Hyways roadmap targets (European Commission 2008) for the best compromise solutions obtained using the proposed multi-objective-MCDM framework. For the sake of illustration, the best solution obtained for hydrogen cost minimization (\$4.18/kg of H₂) and GWP minimization (\$7.30/kg H₂) has also been reported. A consistent approach would be to find a compromise solution between these bounds since the GWP is consistent with the targeted values (Mobilité Hydrogène France 2016) (see Fig. 13).

Fig. 13 compares the well-to-wheel CO₂ emissions per km obtained with FCEVs obtained by the use of the proposed methodology and those related to ICE vehicles equipped with gasoline- or diesel-fuelled engines (Hydrogen Council 2017) for the 2050 period. Currently, on-road fuel economy is approximately 1 kg of hydrogen per 100 km travelled, and the emissions expected for ICE vehicles are approximately 60 g CO₂/km (IEA 2015). With the costs used in the original models, the emissions are in the range of 28 - 38 g CO₂/km for the MILP and GA approaches, respectively. With the new UPC cost, the emissions are less than 20 g CO₂/km. It must be emphasized that FCEV emissions are expected to be less than 23 g CO₂/km (Mobilité Hydrogène France 2016) in 2030, which means that the HSCN obtained with the new costs is competitive with the expected results.

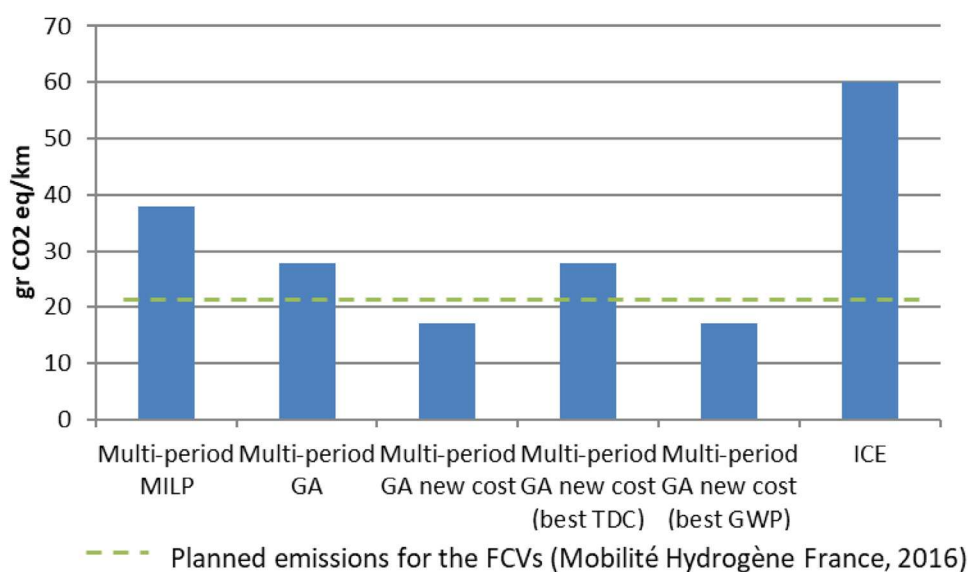


Fig. 13. Comparison of emissions by sector in 2050 (g CO₂/km). Data from [59].

5. Conclusion

This paper has presented the core methodology for HSCN design, combining multi-objective optimization tools and multiple criteria decision-making techniques. The scientific challenge of this work was to use the potential of genetic algorithms as an alternative to the current methodologies in the optimization of the HSC design, particularly as a complementary approach to the MILP framework previously developed in (De-León Almaraz et al., 2014): the size and particularly the number of binary variables have often led to difficulties for problem solution in (De-León Almaraz et al., 2014). In this work, a variant of NSGA-II previously developed in (Gomez et al., 2008) was explored to address the multi-objective formulation so that compromise solutions can be automatically produced.

The case study of the hydrogen mobility market in the former Midi-Pyrénées region has been considered since it was already studied in (De-León Almaraz et al., 2014) for validation purposes of the proposed methodology: it is foreseen to be the fastest growing and most important market in the horizon of 2025 – 2030 and thus is clearly relevant to the context of a “green hydrogen” study.

The objective functions obtained by GA exhibit the same order of magnitude as those obtained with MILP in the mono-criterion problem, and the multi-objective GA yields a Pareto front of better quality with a better distribution of the compromise solutions. However, in our view, both strategies do not have to be opposed, but the maximum use of their potential benefits must be made.

Several experiments were developed with a fixed demand and for mono- and multi-objective cases. In the multi-objective instances, the GA outperforms the ϵ -constraint strategy. It must be emphasized that the GA prioritizes the TDC cost, providing better results than the ϵ -constraint method, as well as the transportation of hydrogen between the grids. The differences in the distributions and the results between the GA and the MILP approaches can be explained by way of managing the constraints and their different logics.

In the original model (De-León Almaraz et al., 2014), the unit production cost (UPC) of electricity remains fixed for all of the periods, regardless of the hydrogen technology, which was a severe simplification. The unit production cost involves the fixed facility costs (maintenance, labour cost), as well as electricity and feed-stock costs, which are more relevant to the reality of costs.

Hydrogen demand was identified as one the most significant parameters for HSCN design, and a GA model was developed with demand uncertainty modelled using fuzzy concepts.

Since hydrogen demand was simply involved through constraints in the HSCN model formulation, the HSC design problem refers to the simplest form of fuzzy linear programming, as proposed by (Verdegay, 1982), (Ebrahimnejad and Verdegay, 2016, Delgado et al., 1993). The solution strategy can thus be easily implemented by varying α , which can be considered the percentage of tolerance added to the base demand. This sensitivity analysis has allowed for identifying more robust solutions. The solutions are compared with the original crisp models, based on either MILP or GA, giving more robustness to the proposed approach.

An extension could be to develop a fuzzy optimization model for supply chain design that considers demand and price uncertainties. The model could be formulated as a fuzzy mixed-integer linear programming model, in which the data are poorly known and modelled by triangular fuzzy numbers. The synergetic effect of genetic algorithms and fuzzy demand modelling could be thus explored so that the fuzzy model would provide the decision maker with alternative decision plans for different degrees of satisfaction.

Finally, this study has revealed that if the economic and environmental criteria can be formulated by proven methodologies, the safety risk is perhaps more difficult to formulate and calibrate.

The use of the framework could be useful in deploying hydrogen solutions since the introduction of hydrogen as an energy carrier is not only a technology challenge, but it also requires the convergence of many economic, environmental and social factors.

Declaration of Competing Interest

All authors have participated in (a) conception and design, or analysis and interpretation of the data; (b) drafting the article or revising it critically for important intellectual content; and (c) approval of the final version. This manuscript has not been submitted to, nor is under review at, another journal or other publishing venue. The authors have no affiliation with any organization with a direct or indirect financial interest in the subject matter discussed in the manuscript.

Supplementary materials

Supplementary material associated with this article can be found, in the online version, at doi:10.1016/j.compchemeng.2020.106853.

Appendix

Indices

g and g'	Grid squares such that $g' \neq g(8)$
l	Product physical form
L	Type of transportation mode
P	Plant type with different production technologies
S	Storage facility type with different storage technologies
E	Energy source type

Parameters

B	Storage holding period - average number of days' worth of stock (days)
γ_{epj}	Rate of utilization of primary energy source e by plant type p and size j (unit resource/unit product)
$AD_{gg'}$	Average delivery distance between g and g' by transportation l (km per trip)
$Ad_{gg'}$	Road risk between grids g and g' (units)
CCF	Capital change factor payback period of capital investment (years)
DT_{ig}	Total demand for product form i in grid g (kg per day)
DW_l	Driver wages for transportation mode l (dollars per hour)
FE_l	Fuel economy of transportation mode l (km per litre)
FP_l	Fuel price of transportation mode l (dollars per litre)
GE_l	General expenses of transportation mode l (dollars per day)
GWP_{prod_p}	Production GWP by plant type p (g CO ₂ -eq per kg of H ₂)
GW_{stock_i}	Storage global warming potential form i (g CO ₂ -eq per kg of H ₂)
GW_{trans_l}	Global warming potential of transportation mode l (g CO ₂ per ton-km)
LUT_l	Load and unload times of product for transportation mode l (hours per trip)
ME_l	Maintenance expenses of transportation mode l (dollars per km)
NOP	Network operating period (days per year)
$Q_{max_{il}}$	Maximum flow rate of product form i by transportation mode l (kg per day)
$Q_{min_{il}}$	Minimum flow rate of product form i by transportation mode l (kg per day)
$PCap_{max_{pi}}$	Maximum production capacity of plant type p for product form i (kg per day)
$PCap_{min_{pi}}$	Minimum production capacity of plant type p for product form i (kg per day)
PCC_{pi}	Capital cost of establishing plant type p producing product form i (dollars)
RP_p	Risk level of the production facility p (units)
RS_s	Risk level of the storage facility s (units)
RT_l	Risk level of the transportation mode l (units)
$SCap_{max_{si}}$	Maximum storage capacity of storage type s for product form i (kg)
$SCap_{min_{si}}$	Minimum storage capacity of storage type s for product form i (kg)
SCC_{si}	Capital cost of establishing storage type s storing product form i (dollars)
SP_l	Average speed of transportation mode l (km per hour)
SSF	Safety stock factor of primary energy sources within a grid (%)
$TCap_{il}$	Capacity of transportation mode l transporting product form i (kg per trip)
TMA_l	Availability of transportation mode l (hours per day)
TMC_{il}	Cost of establishing transportation mode l for product form i (dollars)
UPC_{pi}	Unit production cost for product i produced by plant type p (dollars per kg)
USC_{si}	Unit storage cost for product form i at storage type s (dollar per kg-day)
W_l	Weight of transportation mode l (tons)
WFP_g	Weigh factor risk population in each grid (units)

Variables

A	Rate of utilization of the tolerance
AH_{ig}	Available hydrogen in grid g
DL_{ig}	Demand for product i in grid g satisfied by local production (kg per day)
DI_{ig}	Imported demand for product form i in grid g (kg per day)
FC	Fuel cost (dollars per day)
FCC	Facility capital cost (dollars)
FOC	Facility operating cost (dollars per day)
GC	General cost (dollars per day)
$GWPTot$	Total global warming potential of the network (g CO ₂ -eq per day)
LC	Labour cost (dollars per day)
MC	Maintenance cost (dollars per day)
NPP_{ig}	Number of plants of type p producing product form i in grid g
NSS_{ig}	Number of storage facilities of type s for product form i in grid g
$NTU_{il_{gg'}}$	Number of transport units between g and g'
PD_{ig}	Tolerance of the demand in grid g
$PGWP$	Total daily GWP in production facility p (g CO ₂ -eq per day)
PR_{pig}	Production rate of product i produced by plant type p in grid g (kg per day)
PT_{ig}	Total production rate of product i in grid g (kg per day)
$Q_{il_{gg'}}$	Flow rate of product i by transportation mode l between g and g' (kg per day)
RP_{ig}	Received hydrogen in grid g
$SGWP$	Total daily GWP in the storage technology s (g CO ₂ -eq per day)
SP_{ig}	Overproduction of hydrogen in grid g
ST_{ig}	Total average inventory of product form i in grid g (kg)
TCC	Transportation capital cost (dollars)
TDC	Total daily cost of the network (dollars per day)
$TGWP$	Total daily GWP in transportation mode l (g CO ₂ -eq per day)
TOC	Transportation operating cost (dollars per day)
$TotalRisk$	Total risk of this configuration (units)
$TPRisk$	Total risk index for production activity (units)
$TSRisk$	Total risk index for storage activity (units)
$TTRisk$	Total risk index for transport activity (units)

Model formulation

The model is based on an optimization formulation involving three objective functions (minimization case considered in isolation or simultaneously) and a set of constraints. The constraints are expressed for the whole time horizon divided into several t periods

Cost objective

The cost objective involves the total daily cost (TDC), representing the cost in \$ per day of the entire HSC, in which FCC is the facility capital cost (\$), TCC is the transportation capital cost (\$), and NOP is the network operating period (days per year) related to the capital charge factor (CCF , in years). Then, the facility operating cost (FOC , \$ per day) and the transportation operating cost (TOC , \$ per day) are also associated. In addition, the cost of imported energy (UIC as the unitary imported cost and $IPES$ as the imported energy) is added.

$$TDC = \left(\frac{FCC + TCC}{(NOP)CCF} \right) + FOC + TOC + \sum_{eg} UIC_e IPES_{eg} \quad (A.1)$$

where FCC is related to the establishment of production and storage facilities. It is calculated by the product of the production and storage plants (NP and NS , respectively) and their capital costs (PCC and SCC , respectively), divided by the learning rate, which is a cost reduction for technology and manufacturers that results from the accumulation of experience during a time period.

$$FCC = \sum_{i,g} \left(\frac{1}{LearnR} \left(\sum_p PCC_{pi} NP_{pig} + \sum_s SCC_{si} NS_{sig} \right) \right) \quad (A.2)$$

The transport cost (TCC) depends on the flow rate between different grids (Q), the transportation mode availability (TMA), the distance between grids (AD) (round trip), the average speed (SP), the loading/unloading time (LUT) and the cost for transportation mode (TMC).

$$TCC = \sum_{i,l} \left\{ \left[\sum_{i,l,g,g'} \left(\frac{Q_{i,l,g,g'}}{TMA_l TCap_{il}} \left(\frac{2AD_{gg'}}{SP_l} + LUT_l \right) \right) \right] TMC_{il} \right\} \quad (A.3)$$

FOC refers to the cost for production and storage plant operation, depending on unit production and storage costs (UPC and USC , respectively) and on the quantity of hydrogen produced and stored (PR and ST , respectively).

$$FOC = \sum_{i,g} \left(\sum_p UPC_{pi} PR_{pig} + \sum_s USC_{si} ST_{sig} \right) \quad (A.4)$$

Finally, TOC considers:

- fuel cost (FC), given by the fuel price and the daily fuel usage;
- labour cost (LC), given by the driver wage and the total delivery time;
- maintenance cost (MC), represented by the maintenance of the transportation by distance travelled; and
- and general cost (GC), consisting of transportation insurance, licenses and registrations, and outstanding finances.

$$TOC = FC + LC + MC + GC \quad (A.5)$$

Global warming potential objective

The global warming potential ($GWPTot$, in g CO_2 per day) is given by the total daily production GWP ($PGWP$, in g CO_2 per day), the total daily storage GWP ($SGWP$, in g CO_2 per day) and the total daily transport GWP ($TGWP$, in g CO_2 per day).

$$GWPTOT = PGWP + SGWP + TGWP \quad (A.6)$$

The GWP related to the production is called $PGWP$ and is given by the quantity of hydrogen produced (PR) and the emissions of CO_2 associated with the production facilities (GW_i^{prod}).

$$PGWP = \sum_{pig} (PR_{pig} GW_i^{prod}) \quad (A.7)$$

The GWP associated with the storage is the $SGWP$, where the hydrogen produced (PR) is related to the GWP for the storage technology (GW_i^{stock}).

$$SGWP = \sum_{pig} (PR_{pig} GW_i^{stock}) \quad (A.8)$$

The GWP associated with transport ($TGWP$) is given by the distance (AD) and the flow rate of hydrogen (Q) between grids, the global warming potential (GW_i^{trans}) associated with the transportation mode and its weight (W_1).

$$TGWP = \sum_{i,l,g,g'} \left(\frac{2AD_{l,g,g'} Q_{i,l,g,g'}}{TCap_{il}} \right) GW_i^{Trans} w_l \quad (A.9)$$

Risk objective

The total relative risk (TR) (A.10) compiles $TPRisk$, the total risk of production facilities (A.11), $TSRisk$, the total risk of storage facilities (A.12), and $TTRisk$, the total risk of transportation units (A.13).

$$TR = TPRisk + TSRisk + TTRisk \quad (A.10)$$

Each is computed by the product of the number of production plants (NP) (or the storage units (NS) or the transportation units (NTU)) by a risk factor (RP , RS , and RT , respectively) and by the population weight factor in each grid in which the production or storage facility is located (WFP) or the road risk between grids (Adj).

$$TPRisk = \sum_{pig} (NP_{pig} RP_p WFP_g) \quad (A.11)$$

$$TSRisk = \sum_{sig} (NS_{sig} RS_s WFP_g) \quad (A.12)$$

$$TTRisk = \sum_{i,l,g,g'} NTU_{i,l,g,g'} RT_l Adj_{gg'} \quad (A.13)$$

Constraints

For interoperability purposes with the MULTIGEN platform, the inequality constraints have been coded in Matlab® and formulated following the "lower or equal than zero" structure (≤ 0). All of the demand (DT) must be satisfied with the local production (DL) and the hydrogen imported from other grids (DI)

$$DT_{ig} = DL_{ig} + DI_{ig} \forall i, g \quad (A.14)$$

Based on the conservation of mass, the total flow of hydrogen leaving the grid g (Q , from g to g') and the total production rate in the same grid (PT) must be equal to the flow of hydrogen entering the grid g (Q , from g' to g) and total demand required by the same grid (DT):

$$PT_{ig} = \sum_{l,g'} (Q_{i,l,g,g'} - Q_{i,l,g/g}) + DT_{ig} \forall i, g \quad (A.15)$$

To guarantee the availability of the product, a variable is added. During steady-state operation, the total inventory of product form i in grid g (ST) is equal to a function of the corresponding demand (DT) multiplied by the storage period (β):

$$ST_{ig} = \beta DT_{ig} \forall i, g \quad (A.16)$$

The total amount of hydrogen produced (PT) in each grid must be equal to the hydrogen produced in all of the plants for each grid:

$$PT_{ig} = \sum_p PR_{pig} \forall i, g \quad (A.17)$$

The availability of primary energy sources in each grid (A) is given by the initial average availability of primary energy sources (AO), the importation of energy sources ($IPES$) and the rate of consumption, expressed by the product of the safety stock factor (SSF) and the rate of utilization of primary source (γ) of the production (PR).

$$A_{eg} = AO_{eg} + IPES_{eg} + SSF \sum_{pi} (\gamma_{ep} * PR_{pig}) \quad (A.18)$$

The maximum daily production rate of product form i produced by plant type p is constrained by the number of production facilities NP . Similarly, the total production rate of each product form i in grid g (PT) cannot exceed certain limits. Therefore, PT is bound between the minimum (Eq. A.19) and maximum (Eq. A.20) production capacities of all plants that are established in this particular grid:

$$\sum_p PCap_{pi}^{min} NP_{pig} - PT_{ig} \leq 0 \forall i, g \quad (A.19)$$

$$PT_{ig} - \sum_p PCap_{pi}^{min} NP_{pig} \leq 0 \forall i, g \quad (A.20)$$

Each storage facility (NS) capacity must lie between certain limits and cannot be outside them. This consideration guarantees that the total inventory of each product in each grid is bounded between certain limits, respectively lower (Eq. A.21) and upper bounds (Eq. A.22):

$$\sum_s SCap_{si}^{min} NS_{sig} - ST_{ig} \leq 0 \forall i, g \quad (A.21)$$

$$ST_{ig} - \sum_s SCap_{si}^{min} NS_{sig} \leq 0 \forall i, g \quad (A.22)$$

The production rate of product form i produced by any plant of type p in grid g (PR) cannot exceed a given limit. Thus, there is always a maximum production capacity for any product ($PCap_{pi}^{max}$). Moreover, there is often a minimum production rate ($PCap_{pi}^{min}$) that must be maintained while the plant is operating. Therefore, in the equation (Eq. A.23), PR must be higher than the minimum capacity, but it must be lower than the maximal capacity (Eq. A.24):

$$PCap_{pi}^{min} NP_{pig} - PR_{pig} \leq 0 \forall p, i, g \quad (A.23)$$

$$PR_{pig} - PCap_{pi}^{max} NP_{pig} \leq 0 \forall p, i, g \quad (A.24)$$

The number of refuelling stations within grid g dispensing product form i depends on the total equivalent demand and the installed capacity of the fuelling stations, as follows:

$$NFS = \sum_{i,g} \frac{DT_{ig}}{FCap_i} \quad (A.25)$$

The model requires the unambiguous definition of the hydrogen flow rate and the only way to ensure that hydrogen can be transported (Equations A.26 to A.3), indicating that the demand must be satisfied by hydrogen either produced onsite or imported. Hydrogen in excess must be sent to other grids, or when the demand is not satisfied, it must be fulfilled with hydrogen received from other grids (not the two actions at the same time). In the original model, this goal was achieved using binary variables, thus adding combinatorial complexity, while in this model, some constraints are added to the already existing variables.

All of the overproduction in one city or grid must be sent to other grids (SP) and must fulfil a complete tanker trunk; PT represents the total production and DT the demand in each grid.

$$(PT_{ig} - DT_{ig}) - SP_{ig} = 0 \quad (A.26)$$

The demand in each grid DT must be equal to the available hydrogen AH in the grid (hydrogen produced onsite or imported).

$$DT_{ig} - AH_{ig} = 0 \quad (A.27)$$

In each grid, only one action can be performed, either sending or receiving hydrogen. Then, the next relationship should be satisfied in which RP is the received product type i in grid g

$$\text{Max}(SP_{ig}, RP_{ig}) - (SP_{ig} + RP_{ig}) = 0 \quad (A.28)$$

The total number of production plants (NP) (Eq. A.29) and of storage facilities (NS) (Eq. A.30) in each period is given by the facilities already installed in the previous period and the facilities installed in the given period. s .

$$NP_{pigt} = NP_{pigt-1} + NP_{pigt} \forall p, i, g, t = 1, 2, 3, 4 \quad (A.29)$$

$$NS_{sigt} = NS_{sigt-1} + NS_{sigt} \forall s, i, g, t = 1, 2, 3, 4 \quad (A.30)$$

Each grid has its own demand that must be satisfied with hydrogen produced in the same grid or with hydrogen imported from other grids. Therefore, the contribution of the demand satisfied with hydrogen produced in the same grid (DL) is given by:

$$DL_{ig} - PT_{ig} \leq 0 \forall i, g \quad (A.31)$$

References

- Almansoori, A., Shah, N., 2006. Design and Operation of a Future Hydrogen Supply Chain: Snapshot Model. *Chem. Eng. Res. Des.* 84 (6), 423–438 Jun.
- Almansoori, A., Shah, N., 2012. Design and operation of a stochastic hydrogen supply chain network under demand uncertainty. *Int. J. Hydrog. Energy* 37 (5), 3965–3977.
- Bento, N., 'La transition vers une économie de l'hydrogène: infrastructures et changement technique', Université Pierre Mendès-France-Grenoble II, 2010.
- Chen, C.-L., Lee, W.-C., 2004. Multi-objective optimization of multi-echelon supply chain networks with uncertain product demands and prices. *Comput. Chem. Eng.* 28 (6), 1131–1144.
- Dagdougui, H., Ouammi, A., Sacile, R., 2012. Modelling and control of hydrogen and energy flows in a network of green hydrogen refuelling stations powered by mixed renewable energy systems. *Int. J. Hydrog. Energy* 37 (6), 5360–5371 Mar.
- De León Almaraz, S., 'Multi-objective optimisation of a hydrogen supply chain', 14-Feb- 2014. [Online]. Available: <http://ethesis.inp-toulouse.fr/archive/00002723/>. [Accessed: 5-July-2019].
- De-León Almaraz, S., Azzaro-Pantel, C., Montastruc, L., Domenech, S., 2014. Hydrogen supply chain optimization for deployment scenarios in the Midi-Pyrénées region, France. *Int. J. Hydrog. Energy* 39 (23), 11831–11845.
- Deb, K., Pratap, A., Agarwal, S., Meyarivan, T., 2002. A fast and elitist multiobjective genetic algorithm: NSGA-II. *Evol. Comput. IEEE Trans. On* 6 (2), 182–197.
- Delgado, M., Herrera, F., Verdegay, J.L., Vila, M.A., 1993. Post-optimality analysis on the membership functions of a fuzzy linear programming problem. *Fuzzy Sets Syst.* 53 (3), 289–297 Feb.
- Dimopoulos, C., Zalzal, A.M.S., 2000. Recent developments in evolutionary computation for manufacturing optimization: problems, solutions, and comparisons. *IEEE Trans. Evol. Comput.* 4 (2), 93–113.
- Ebrahimnejad, A., Verdegay, J.L., 2016. A Survey on Models and Methods for Solving Fuzzy Linear Programming Problems. in *Fuzzy Logic in Its 50th Year*. Springer, Cham, pp. 327–368.
- Eskandarpour, M., Dejax, P., Miemczyk, J., Péton, O., 2015. Sustainable supply chain network design: An optimization-oriented review. *Omega* 54, 11–32.
- European Commission, 2008. HyWays the European Hydrogen Roadmap. EUR 23123.
- Gen, M. and Cheng, R., *Genetic Algorithms and Engineering Optimization*. John Wiley & Sons, 2000.
- Gomez, A., Azzaro-Pantel, C., L.Pibouleau, and Domenech, S., 'Teaching Mono and Multi-objective Genetic Algorithms in Process Systems Engineering: an illustration with the MULTIGEN environment, ESCAPE 18', in 18th European Symposium on Computer Aided Process Engineering, ESCAPE, 2008, vol. 18.
- Govindan, K., Fattahi, M., Keyvanshokoh, E., 2017. Supply chain network design under uncertainty: A comprehensive review and future research directions. *Eur. J. Oper. Res.* 263 (1), 108–141.
- Guillén-Gosálbez, G., Mele, F.D., Grossmann, I.E., 2010. A bi-criterion optimization approach for the design and planning of hydrogen supply chains for vehicle use. *AIChE J.* 56 (3), 650–667.

- Hydrogen Council, 'Hydrogen scaling up. A sustainable pathway for the global energy transition', Nov- 2017. [Online]. Available: <http://hydrogencouncil.com/wp-content/uploads/2017/11/Hydrogen-scaling-up-Hydrogen-Council.pdf>. [Accessed: 04-Jan-2018].
- IEA, 'Technology Roadmap. Hydrogen and Fuel Cells', 2015. [Online]. Available: <https://www.iea.org/publications/freepublications/publication/TechnologyRoadmapHydrogenandFuelCells.pdf>. [Accessed: 31-Dec-2017].
- IEA, 'International Energy Agency Technical Report. Key world energy statistics', Sep- 2017. [Online]. Available: <https://www.iea.org/publications/freepublications/publication/KeyWorld2017.pdf>. [Accessed: 29-Dec-2017].
- Jung, J.Y., Blau, G., Pekny, J.F., Reklaitis, G.V., Eversdyk, D., 2004. A simulation based optimization approach to supply chain management under demand uncertainty. *Comput. Chem. Eng.* 28 (10), 2087–2106.
- Kim, J., Moon, I., 2008. Strategic design of hydrogen infrastructure considering cost and safety using multiobjective optimization. *Int. J. Hydrog. Energy* 33 (21), 5887–5896 Nov.
- Kim, J., Lee, Y., Moon, I., 2008. Optimization of a hydrogen supply chain under demand uncertainty. *Int. J. Hydrog. Energy* 33 (18), 4715–4729.
- Kim, J., Lee, Y., Moon, I., 2011. An index-based risk assessment model for hydrogen infrastructure. *Int. J. Hydrog. Energy* 36 (11), 6387–6398 Jun.
- Mavrotas, G., 'Generation of efficient solutions in Multiobjective Mathematical Programming problems using GAMS. Effective implementation of the ϵ -constraint method', Lect. Lab. Ind. Energy Econ. Sch. Chem. Eng. Natl. Tech. Univ. Athens, 2007.
- McKinsey & Company, 'A portfolio of power-trains for Europe: a fact-based analysis. The role of Battery Electric Vehicles, Plug-in Hybrids and Fuel Cell Electric Vehicles', 2010.
- McKinsey & Company, A., portfolio of power-trains for Europe: a fact-based analysis. Report, 2010.
- Mobilité Hydrogène France, 'H2 MOBILITÉ FRANCE. Study for a Fuel Cell Electric Vehicle national deployment plan', 2016. [Online]. Available: <http://www.fch.europa.eu/sites/default/files/Smart%20Spec%20Fabio%20Ferrari%20%28ID%202436338%29%20%28ID%202497336%29.pdf>. [Accessed: 31-Dec-2017].
- Murthy Konda, N., Shah, N., Brandon, N.P., 2011. Optimal transition towards a large-scale hydrogen infrastructure for the transport sector: the case for the Netherlands. *Int. J. Hydrog. Energy* 36 (8), 4619–4635.
- Nunes, P., Oliveira, F., Hamacher, S., Almansoori, A., 2015. Design of a hydrogen supply chain with uncertainty. *Int. J. Hydrog. Energy* 40 (46), 16408–16418 Dec.
- Ochoa Robles, J., Azzaro-Pantel, C., De-Leon Almaraz, S., 2015. Design of experiments for sensitivity analysis in multi-objective optimization of hydrogen supply chain. in 28th International conference on Efficiency, Cost, Optimization, Simulation and Environmental Impact of Energy Systems. ECOS 2015.
- Ochoa Robles, J., De-León Almaraz, S., and Azzaro-Pantel, C., 'Design of Experiments for Sensitivity Analysis of a Hydrogen Supply Chain Design Model', *Process Integr. Optim. Sustain.*, pp. 1–22, Dec. 2017.
- Ochoa Robles, J., Azzaro-Pantel, C., De-Leon Almaraz, S., 2018. Hydrogen Supply Chain Design: key technological components and sustainable assessment. In: in Design, Deployment and Operation of a Hydrogen Supply Chain, 1st Edition.. Catherine Azzaro-Pantel, p. 352.
- Ren, L., Zhang, Y., Wang, Y., and Sun, Z., 'Comparative analysis of a novel M-TOPSIS method and TOPSIS', *Appl. Math. Res. EXpress*, vol. 2007, p. abm005, 2007.
- Sabio, N., Gadalla, M., Guillén-Gosálbez, G., Jiménez, L., 2010. Strategic planning with risk control of hydrogen supply chains for vehicle use under uncertainty in operating costs: a case study of Spain. *Int. J. Hydrog. Energy* 35 (13), 6836–6852.
- Verdegay, J.L., 1982. Fuzzy mathematical programming. *Fuzzy Inf. Decis. Process.* 231, 237.
- Villacorta, P.J., Rabelo, C.A., Pelta, D.A., Verdegay, J.L., 2017. FuzzyLP: An R Package for Solving Fuzzy Linear Programming Problems. In: in Granular, Soft and Fuzzy Approaches for Intelligent Systems. Springer, Cham, pp. 209–230.
- You, F., Grossmann, I.E., 2008. Design of responsive supply chains under demand uncertainty. *Comput. Chem. Eng.* 32 (12), 3090–3111.